

**AFRL-ML-WP-TR-2001-4016**

**INTRINSICALLY SURVIVABLE  
STRUCTURAL  
COMPOSITE MATERIALS**

**DAVID P. ANDERSON  
CHENGGANG CHEN  
LARRY CLOOS  
THAO GIBSON**



**UNIVERSITY OF DAYTON RESEARCH INSTITUTE  
300 COLLEGE PARK AVENUE  
DAYTON, OH 45469-0168**

**FEBRUARY 2001**

**FINAL REPORT FOR PERIOD 15 SEPTEMBER 1999 – 31 JULY 2000**

**APPROVED FOR PUBLIC RELEASE; DISTRIBUTION UNLIMITED.**

**MATERIALS AND MANUFACTURING DIRECTORATE  
AIR FORCE RESEARCH LABORATORY  
AIR FORCE MATERIEL COMMAND  
WRIGHT-PATTERSON AIR FORCE BASE, OH 45433-7750**

## REPORT DOCUMENTATION PAGE

<b>1. REPORT DATE (DD-MM-YYYY)</b> 01-02-2001	<b>2. REPORT TYPE</b> Final	<b>3. DATES COVERED (FROM - TO)</b> 15-09-1999 to 31-07-2000
<b>4. TITLE AND SUBTITLE</b> Intrinsically survivable Structural Composite Materials  Unclassified		<b>5a. CONTRACT NUMBER</b>
		<b>5b. GRANT NUMBER</b>
		<b>5c. PROGRAM ELEMENT NUMBER</b>
<b>6. AUTHOR(S)</b> Anderson, David P. ; Chen, Chenggang ; Cloos, Larry ; Gibson, Thao ;		<b>5d. PROJECT NUMBER</b>
		<b>5e. TASK NUMBER</b>
		<b>5f. WORK UNIT NUMBER</b>
<b>7. PERFORMING ORGANIZATION NAME AND ADDRESS</b> University of Dayton Research Institute 300 College Park Ave.  Dayton , OH 45469-0168		<b>8. PERFORMING ORGANIZATION REPORT NUMBER</b>
<b>9. SPONSORING/MONITORING AGENCY NAME AND ADDRESS</b> Materials and Manufacturing Directorate Air Force Research Laboratory Air Force Materiel Command Wright-Patterson AFB , OH 45433-7750		<b>10. SPONSOR/MONITOR'S ACRONYM(S)</b>
		<b>11. SPONSOR/MONITOR'S REPORT NUMBER(S)</b>
<b>12. DISTRIBUTION/AVAILABILITY STATEMENT</b> A PUBLIC RELEASE  Materials and Manufacturing Directorate Air Force Research Laboratory Air Force Materiel Command Wright-Patterson AFB , OH 45433-7750		

<b>13. SUPPLEMENTARY NOTES</b>
<b>14. ABSTRACT</b> Three aspects of nanocomposite materials were examined in this project: spherical silicates, commercial layered silicates, and synthetically modified layered silicates. Aerospace epoxy resins were used throughout with primary focus on the resin transfer molding (RTM) grade Epon 862/Cure W.
<b>15. SUBJECT TERMS</b>

<b>16. SECURITY CLASSIFICATION OF:</b>			<b>17. LIMITATION OF ABSTRACT</b> Public Release	<b>18. NUMBER OF PAGES</b> 51	<b>19a. NAME OF RESPONSIBLE PERSON</b> Fenster, Lynn lfenster@dtic.mil
<b>a. REPORT</b> Unclassified	<b>b. ABSTRACT</b> Unclassified	<b>c. THIS PAGE</b> Unclassified			<b>19b. TELEPHONE NUMBER</b> International Area Code  Area Code Telephone Number 703 767-9007 DSN 427-9007

## REPORT DOCUMENTATION PAGE

<b>1. REPORT DATE (DD-MM-YYYY)</b> 01-02-2001	<b>2. REPORT TYPE</b> Final	<b>3. DATES COVERED (FROM - TO)</b> 15-09-1999 to 31-07-2000
<b>4. TITLE AND SUBTITLE</b> Intrinsically survivable Structural Composite Materials  Unclassified	<b>5a. CONTRACT NUMBER</b>	
	<b>5b. GRANT NUMBER</b>	
	<b>5c. PROGRAM ELEMENT NUMBER</b>	
<b>6. AUTHOR(S)</b> Anderson, David P. ; Chen, Chenggang ; Cloos, Larry ; Gibson, Thao ;	<b>5d. PROJECT NUMBER</b>	
	<b>5e. TASK NUMBER</b>	
	<b>5f. WORK UNIT NUMBER</b>	
<b>7. PERFORMING ORGANIZATION NAME AND ADDRESS</b> University of Dayton Research Institute 300 College Park Ave.  Dayton , OH 45469-0168	<b>8. PERFORMING ORGANIZATION REPORT NUMBER</b>	
<b>9. SPONSORING/MONITORING AGENCY NAME AND ADDRESS</b> Materials and Manufacturing Directorate Air Force Research Laboratory Air Force Materiel Command Wright-Patterson AFB , OH 45433-7750	<b>10. SPONSOR/MONITOR'S ACRONYM(S)</b>	
	<b>11. SPONSOR/MONITOR'S REPORT NUMBER(S)</b>	
<b>12. DISTRIBUTION/AVAILABILITY STATEMENT</b> A PUBLIC RELEASE  Materials and Manufacturing Directorate Air Force Research Laboratory Air Force Materiel Command Wright-Patterson AFB , OH 45433-7750		

<b>13. SUPPLEMENTARY NOTES</b>
<b>14. ABSTRACT</b> Three aspects of nanocomposite materials were examined in this project: spherical silicates, commercial layered silicates, and synthetically modified layered silicates. Aerospace epoxy resins were used throughout with primary focus on the resin transfer molding (RTM) grade Epon 862/Cure W.
<b>15. SUBJECT TERMS</b>

<b>16. SECURITY CLASSIFICATION OF:</b>			<b>17. LIMITATION OF ABSTRACT</b> Public Release	<b>18. NUMBER OF PAGES</b> 51	<b>19a. NAME OF RESPONSIBLE PERSON</b> Fenster, Lynn lfenster@dtic.mil
<b>a. REPORT</b> Unclassified	<b>b. ABSTRACT</b> Unclassified	<b>c. THIS PAGE</b> Unclassified			<b>19b. TELEPHONE NUMBER</b> International Area Code  Area Code Telephone Number 703 767-9007 DSN 427-9007

## NOTICE

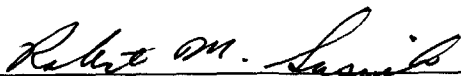
Using government drawings, specifications, or other data included in this document for any purpose other than government procurement does not in any way obligate the US Government. The fact that the government formulated or supplied the drawings, specifications, or other data does not license the holder or any other person or corporation or convey any rights or permission to manufacture, use, or sell any patented invention that may relate to them.

This report is releasable to the National Technical Information Service (NTIS). At NTIS, it will be available to the general public, including foreign nations.

This technical report has been reviewed and is approved for publication.



L. SCOTT THEIBERT, Chief  
Structural Materials Branch  
Nonmetallic Materials Division



ROBERT M. SUSNIK, Assistant Chief  
Nonmetallic Materials Division  
Materials and Manufacturing Directorate

Do not return copies of this report unless contractual obligations or notice on a specific document requires its return.

REPORT DOCUMENTATION PAGE			Form Approved OMB No. 0704-0188		
<p>The public reporting burden for this collection of information is estimated to average 1 hour per response, including the time for reviewing instructions, searching existing data sources, gathering and maintaining the data needed, and completing and reviewing the collection of information. Send comments regarding this burden estimate or any other aspect of this collection of information, including suggestions for reducing the burden, to Department of Defense, Washington Headquarters Services, Directorate for Information Operations and Reports (0704-0188), 1215 Jefferson Davis Highway, Suite 1204, Arlington, VA 22202-4302. Respondents should be aware that notwithstanding any other provision of law, no person shall be subject to any penalty for failing to comply with a collection of information if it does not display a currently valid OMB control number.</p> <p><b>PLEASE DO NOT RETURN YOUR FORM TO THE ABOVE ADDRESS.</b></p>					
1. REPORT DATE (DD-MM-YYYY) FEBRUARY 2001		2. REPORT TYPE FINAL REPORT		3. DATES COVERED (From - To) 09/15/1999 - 07/31/2000	
4. TITLE AND SUBTITLE INTRINSICALLY SURVIVABLE STRUCTURAL COMPOSITE MATERIALS			5a. CONTRACT NUMBER F33615-95-D-5029		
			5b. GRANT NUMBER		
			5c. PROGRAM ELEMENT NUMBER 62102F		
6. AUTHOR(S) DAVID P. ANDERSON, CHENGGANG CHEN, LARRY CLOOS, AND THAO GIBSON			5d. PROJECT NUMBER 4347		
			5e. TASK NUMBER 34		
			5f. WORK UNIT NUMBER 10		
7. PERFORMING ORGANIZATION NAME(S) AND ADDRESS(ES) UNIVERSITY OF DAYTON RESEARCH INSTITUTE 300 COLLEGE PARK AVENUE DAYTON, OH 45469-0168			8. PERFORMING ORGANIZATION REPORT NUMBER UDR-TR-2000-00112		
9. SPONSORING/MONITORING AGENCY NAME(S) AND ADDRESS(ES) MATERIALS AND MANUFACTURING DIRECTORATE AIR FORCE RESEARCH LABORATORY AIR FORCE MATERIEL COMMAND WRIGHT-PATTERSON AFB, OH 45433-7750			10. SPONSOR/MONITOR'S ACRONYM(S) AFRL/MLBC		
			11. SPONSOR/MONITOR'S REPORT NUMBER(S) AFRL-ML-WP-TR-2001-4016		
12. DISTRIBUTION/AVAILABILITY STATEMENT APPROVED FOR PUBLIC RELEASE; DISTRIBUTION UNLIMITED.					
13. SUPPLEMENTARY NOTES					
14. ABSTRACT Nanosilicate composite materials were examined in this project in the form of spherical silicates, commercial layered silicates, and synthetically modified, layered silicates. Aerospace epoxy resins were used throughout with primary focus on the RTM grade Epon 862/Cure W. The spherical silicates ranged in size from 7- to 33-nm diameters and used acetone or methanol dispersants. While a moderate increase in fracture toughness was observed, work was discontinued in favor of the layered-silicate research. The commercial layered-silicate composites showed a decrease in their one-dimensional binary diffusion coefficient of water but suffered from a flocculation problem. Lower temperature curing, high-shear mixing, and a chemical activator were unable to overcome the commercial clay inconsistencies. Consistently exfoliated nanocomposites have been prepared from chemically modified organosilicate clays. Compared to the neat resin, these nanocomposites have lower thermal expansion coefficients, higher dynamic mechanical analysis storage modulus and static modulus with somewhat reduced fracture toughness and flex strength, while retaining the reduced binary diffusion coefficient of the commercial clay nanocomposites. Future activities in this area should focus on the development of functionalized organosilicate clays which will promote covalent bonds with the host matrix.					
15. SUBJECT TERMS Composites, nanocomposites, epoxy composites, epoxy resins, clays, silicates, layered silicates, synthetic silicates, silane modified, organoclays, x-ray diffraction, TEM, mechanical properties, CTE					
16. SECURITY CLASSIFICATION OF:			17. LIMITATION OF ABSTRACT	18. NUMBER OF PAGES	19a. NAME OF RESPONSIBLE PERSON
a. REPORT U	b. ABSTRACT U	c. THIS PAGE U	SAR	51	L. SCOTT THEIBERT/AFRL/MLBC
					19b. TELEPHONE NUMBER (Include area code) 937/255-9070

Standard Form 298 (Rev. 8/98)  
Prescribed by ANSI Std. Z39.18

## CONTENTS

Section		Page
	<b>EXECUTIVE SUMMARY</b>	<b>1</b>
<b>1</b>	<b>SPHERICAL SILICATE COMPOSITES</b>	<b>3</b>
	1.1 INTRODUCTION	3
	1.2 MATERIALS	3
	1.3 EXPERIMENTAL PROCEDURE	4
	1.4 RESULTS AND DISCUSSION	7
	1.5 CONCLUSIONS AND RECOMMENDATIONS	13
<b>2</b>	<b>COMMERCIAL LAYERED-SILICATE COMPOSITES</b>	<b>14</b>
	2.1 INTRODUCTION	14
	2.2 EXPERIMENTAL PROCEDURES AND RESULTS	14
	2.2.1 Characterization of S30A: One-Dimensional Binary Diffusion Coefficient	14
	2.2.2 Low-Temperature Precure Treatment (LTPT)	16
	2.2.3 Investigation of Several Commercially Available Organoclays	18
	2.2.4 High-Shear Mixing and the Addition of a Chemical Activator	19
	2.3 CONCLUSIONS	20
<b>3</b>	<b>SYNTHETICALLY MODIFIED LAYERED-SILICATE COMPOSITES</b>	<b>23</b>
	3.1 INTRODUCTION	23
	3.2 EXPERIMENTAL PROCEDURES	24
	3.2.1 Materials	24
	3.2.2 Preparation	25
	3.2.3 Processing	25
	3.2.4 Characterization	26



## **CONTENTS (Concluded)**

<b>Section</b>		<b>Page</b>
	3.3 RESULTS AND DISCUSSION	27
	3.3.1 Organosilicates	27
	3.3.2 Epoxy-Silicate Nanocomposites	29
	3.4 CONCLUSIONS	38
<b>4</b>	<b>PUBLICATIONS AND PRESENTATIONS</b>	<b>39</b>
<b>5</b>	<b>REFERENCES</b>	<b>40</b>
	<b>LIST OF ACRONYMS</b>	<b>42</b>

## FIGURES

Figure		Page
1	Fracture Toughness of 33-nm Sized Particles with or without Silane used on Different Particle Concentrations	9
2	Fracture Toughness as a Function of Particle Size	9
3	Fracture Toughness of 14-nm Sized Particles with Concentrations in a Range of 0 to 3%	10
4	Flexure Modulus and Flexure Strength of Nanocomposite Panels	12
5	Scanning Electron Micrograph of 1% Silica, 14-nm Sized Panel: TG766-27S	13
6	Mass Gains versus the Square Root of Time for the Clay Nanocomposites	15
7	Viscosity-Time Data for 1% S30A-Epon 862-W	17
8	The TEM Micrograph of the Epoxy- Nanocomposite of 3% SC16/Epon 862/W	33
9	The Viscosity of the Epon 862 Resin and Curing Agent W with Various Clay (I.30E) Loadings (0%, 1%, 3% and 5%)	35
10	Uptake of 6% SC16/Epon 862/W and Epon 862/W (Control) in Methanol	38

## TABLES

Table		Page
1	Types and Sources of Silicon Dioxide Particles	4
2	Nanocomposite Panels Descriptions	5
3	Mechanical Data of Control Panels	7
4	Mechanical Results of Nanocomposite Panels Containing 33-nm Spherical Particles	8
5	Mechanical Properties of Nanocomposite Panels Containing 14-nm and 7-nm Particles	10
6	Mechanical Results of the Suspension Particle and the Gel Particle Panels	11
7	Glass Transition Temperature of 33-nm Particles	12
8	Composite Samples Prepared Using S30A Clay	15
9	Diffusion Coefficients for Each of the Composite Specimens from Figure 6	16
10	Sample Cure Cycles and Processing Observations for Small Clay Epoxy Samples	17
11	Sample Cure Cycles and Processing Observations for Small Clay Epoxy Samples	18
12	S30A Clay Composites Prepared Using High-Shear Mixing and a Chemical Activator	19
13	Average Diffusion Coefficients for S30A/Epon 862	20
14	XRD Results for Nanocomposites made from Commercial and Synthesized Organosilicates	29
15	Composition, XRD Characterization and Optical Appearance of the Nanocomposites	30
16	Composition, SAXS Data of the Nanocomposites from Rigaku RU-200 and National Synchrotron Light Source	32

## **TABLES (Concluded)**

<b>Table</b>		<b>Page</b>
17	Thermal Expansion Coefficients of the Nanocomposites and Their Pristine Polymers	34
18	Storage Moduli and Glass Transition Temperatures (T <sub>g</sub> ) of the Nanocomposites and Their Pristine Polymers from Dynamic Mechanical Analysis	36
19	Mechanical Properties of Nanocomposites	37
20	Compact Tension Test Results from Nanocomposites at -250°F	37

## **FOREWORD**

This report was prepared by the University of Dayton Research Institute under Air Force Contract No. F33615-95-D-5029, Delivery Order No. 0005. The work was administered under the direction of the Nonmetallic Materials Division, Materials and Manufacturing Directorate, Air Force Research Laboratory, Air Force Materiel Command, with Mr. L. Scott Theibert (AFRL/MLBC) as Project Engineer.

This report was submitted in November 2000 and covers work conducted from 15 September 1999 through 31 July 2000.

## EXECUTIVE SUMMARY

Three aspects of nanocomposite materials were examined in this project: spherical silicates, commercial layered silicates, and synthetically modified layered silicates. Aerospace epoxy resins were used throughout with primary focus on the resin transfer molding (RTM) grade Epon 862/Cure W.

Several sizes of spherical silicon dioxide nanosized particles and solvents serving as dispersion media were examined. No flocculation was observed on 7-nm and 14-nm sized particles using acetone as a dispersant. Fracture toughness of the composites containing 14-nm sized particles at a two-percent loading showed an increase of 15 percent over control panels with no particles. The fracture toughness was observed to be improved as the weight fraction of particles increased from one to two percent. For 33-nm sized particles, where methanol was used as a suspension media, the fracture toughness did not improve with increased silica concentration or with the addition of a silane coupling agent. Flexure strength and flexure moduli were not affected by changes in particle size, silane addition, or particle concentrations using spherical silica.

Commercial layered silicate (S30A) composites (862/W) showed a decrease in their one-dimensional binary diffusion coefficient for water with respect to the pristine resin matrix as the clay loading increased up to five percent. An increase of almost 12 percent at 40°C and over 16 percent at 65°C was observed. This work also suggests that successful incorporation of a layered silicate into a polymer matrix depends to a great extent on the polarities of each component. The inability to successfully incorporate S30A into Epon 862 consistently is most likely the result of manufacturer inconsistencies. In all trials the flocculation did not occur until the final curing stage. That is, the preparation of the nanocomposite material resulted in a visually homogeneous

solution (although the morphology of the system was unknown) until the sample was put through its curing cycle. Attempts to lock the S30A into place by curing at lower temperatures were successful in small batches but could not be scaled to larger amounts of material. Additional commercially available organoclay samples all flocculated to a greater extent than the original S30A. Other attempts to reduce flocculation by the introduction of high-shear mixing and a chemical activator such as acetone were also unsuccessful. Chemically modified clays appear to hold the most promise.

The chemically modified clays SC18, SC16 and I.30E had the best compatibility with epoxy resin to form the nanocomposites. A series of epoxy-organosilicate nanocomposites have been successfully prepared with the nanosheets of the nano-organoclay uniformly and homogeneously distributed in the epoxy resin. The optically transparent or translucent nanocomposites have wide-angle x-ray diffraction and small-angle x-ray scattering patterns, which demonstrates that the nanocomposites are exfoliated. Transmission electron microscopy of the nanocomposites confirms that the organoclay was very well dispersed and exfoliated in the epoxy resin. The thermal expansion coefficients of the nanocomposites are generally lower than those of the pristine epoxy resin. The dynamic mechanical analysis demonstrates that the storage modulus is higher than that of the pure epoxy resin. The mechanical tests show that the modulus of the nanocomposite is higher than that of the pristine epoxy resin, while the fracture toughness and flex strength are reduced to some extent. The solvent uptake of the nanocomposites is reduced compared with the pure epoxy resin.

## **1. SPHERICAL SILICATE COMPOSITES**

### **1.1 INTRODUCTION**

Nanoscale-reinforced polymeric composites, or nanocomposites, have been shown to offer tremendous improvements in mechanical and physical properties at very low loading levels for a number of polymeric resins [1-3]. Nanoscale filled aerospace resins have been developed with a significant improvement in fracture toughness at low volume fractions of nanoscale filler particles. However, as fracture toughness is very sensitive to morphology, the composite processing and effective dispersion of particles is critical in this system [4,5]. Such low loadings enable conventional polymer processes, such as injection molding, and potential matrix modifications for fiber-reinforced composites. In our studies we varied the weight fraction of silicon dioxide using levels of 0.5, 1.0, 2.0, and 3.0 percent as well as varied particle sizes. We evaluated the effectiveness of different suspension media, such as methanol and acetone, in dispersing particles prior to the addition of the particles to the epoxy resin.

### **1.2 MATERIALS**

Shell Epon 862, a low-viscosity bisphenol F/epichlorohydrin-based liquid epoxy resin, and curing agent Cure W, diethyltoluenediamine, were used in this study. The Z-6040 silane coupling agent (3-glycidoxypropyltrimethoxy silane) from Dow Corning was also used. Silicon dioxide was obtained from different sources as fumed powders and colloidal suspensions as shown in Table 1. Methanol and acetone certified by the American Chemical Society (ACS) were obtained from Fisher Scientific.



**Table 1**  
**Types and Sources of Silicon Dioxide Particles**

<b>Particle sizes</b>	<b>Types</b>	<b>Sources</b>
5 $\mu\text{m}$	Spherical, fumed	US silica Min-U-Sil
33 nm	Spherical, fumed	Nanophase NanoTek
20 nm and 30 nm	Gel	Ohio State University
20 nm , 40% in water	Colloidal dispersion	Alfa Aesar
14 nm and 7 nm	Fumed	Aldrich Chemical

### **1.3 EXPERIMENTAL PROCEDURE**

Several solvents were evaluated for their ability to be used as dispersants for the nanosized silicon dioxide particles. Methanol and acetone, nontoxic volatile solvents which were easy to remove by vacuum at 60°C, were used. Methanol was used for the 33 nm and 5  $\mu\text{m}$  particles, and acetone was chosen for use with 7-nm and 14-nm particles. The nanocomposite panels made are described in Table 2.

Having two dispersion media required two mixing methods. For the methanol systems, 500-g batches of resin were made. These were typical 80 percent epoxy, 20 percent cure W, and 0.3 percent silane couple agent by weight. The first 10 panels were made with 33-nm and 5- $\mu\text{m}$  particles. Approximately 150-200 ml of methanol were measured into a reactor flask fitted with a three-neck head and placed in a model 8852 ultrasonic water bath held at 60°C. The silicon-dioxide particles were added to the methanol along with 3-5 g of the epoxy resin. The mixture was then mixed at maximum speed with a banana blade stirring rod driven by a 1/20-horsepower motor connected with a #13530-10 solid-state dual power control set on maximum. In some cases 1 mL of water was added to the mixture when silane coupling agent was used. Also shown in Table 2, panel TG766-10 had silane but no water added, and panel TG766-9 had water but no silane. After 30 minutes the remaining epoxy was added to the mixture, and the entire resin system was stirred for an additional one to two hours. The resin

**Table 2**  
**Nanocomposite Panels Descriptions**

<b>Panel #</b>	<b>Particle Size</b>	<b>% Particles</b>	<b>Silane</b>	<b>Mixing Time</b>	<b>Solvent Used</b>	<b>Comments</b>
TG766-3	33 nm	0.5	no	6 hr	Methanol	
TG766-6	33 nm	1	no	3.5 hr	Methanol	
TG766-5	33 nm	2	no	3 hr	Methanol	
TG766-4	33 nm	0.5	yes	3.5 hr	Methanol	
TG766-7	33 nm	1	yes	3.5 hr	Methanol	
TG766-8	33 nm	2	yes	3 hr	Methanol	
TG766-9	33 nm	1	no	3 hr	Methanol	water added
TG766-10	33 nm	1	yes	3 hr	Methanol	no water added
TG766-11	33 nm	1	no	2 hr	Methanol	
TG766-12	5 nm	1	yes	3 hr	Methanol	
TG766-19	20 nm	1	yes	8 hr	Acetone	colloidal silica in 40% H <sub>2</sub> O
TG766-25	30 nm	1	no	4 hr	Acetone	silica gel, OSU particles
TG766-26S	20 nm	1	yes	4 hr	Acetone	silica gel, OSU particles
TG766-27S	14 nm	1	yes	overnight	Acetone	no water added
TG766-30	14 nm	1.5	yes	overnight	Acetone	no water added
TG766-30-A	14 nm	2	yes	overnight	Acetone	no water added
TG766-32	14 nm	2	yes	overnight	Acetone	
TG766-34	14 nm	1	yes	overnight	Acetone	
TG766-36	14 nm	1.5	yes	overnight	Acetone	
TG766-38-A	14 nm	2	yes	3 hr	Acetone	
TG766-38-B	-	0	yes	3 hr	NA	
TG766-38-C	-	0	no	3 hr	NA	
TG766-40-A	7 nm	2	yes	7 hr	Acetone	
TG766-40-B	14 nm	2	no	7 hr	Acetone	
TG766-42	-	0	no	30 min	NA	
TG766-43-A	14 nm	3	no	overnight	Acetone	
TG766-43-B	14 nm	3	no	overnight	Acetone	Compact tension tested at -250°F
TG766-43-C	14 nm	3	no	overnight	Acetone	postcure for 1 hr @ 350°F
TG766-43-D	14 nm	3	no	overnight	Acetone	postcure for 1 hr @350°F, compact tension tested at -250°F

Note: NA = not available.

mixture was then evacuated for another one to two hours to remove the methanol. Finally, cure W was added, and the resin mixture was stirred for 30 more minutes and then cast into a panel.

The second mixing method using acetone was slightly different. At the beginning of the mixing process, silicon-dioxide particles and acetone were mixed with a magnetic stirring bar in a 1000-mL beaker for 30-60 minutes. A mixture of epoxy and acetone was prepared at the same time. Epoxy was poured into the reaction flask and placed in the ultrasonic water bath held at

60°C as in the first method. Approximately 600 mL of acetone was used for every 500 g of epoxy and curing agent. The amount of acetone added to the epoxy was approximately 50-100 mL. The silicon dioxide particle dispersion was added to the epoxy/acetone mixture and stirred for 1-2 hours. The acetone was then removed by vacuum for at least four hours and sometimes overnight with mixing. Cure W curing agent was added and mixed for 30 minutes before casting the panel.

Control panels which did not contain particles or solvents were made as controls. The epoxy was stirred in an Erlenmeyer flask with a magnetic stirrer for 30 minutes in a water bath at 60°C. Cure W curing agent was then added to the epoxy, and the mixture was evacuated to degas the resin for 15 minutes before casting. Panel TG766-38-B contained silane coupling agent.

Regardless of the mixing method, the resin batches were molded between glass plates with a 1/4-inch gap and cured in the programmable Blue M oven. A 1/4-inch-thick silicon rubber gasket was used to set the mold gap. The curing cycle consisted of a 30-minute ramp from ambient to 250°F, a two-hour hold at 250°F, a 30-minute ramp from 250°F to 350°F, and two-hour hold at 350°F. The panel was cooled from 350°F to ambient temperature over two hours.

Fracture toughness was measured by ASTM E399 compact tension test, with a crosshead travel rate of 0.05 in/min at ambient conditions. Samples containing 3.0 percent loading silicon dioxide particles were tested at a low temperature of -250°F condition. The specimens were machined to dimensions of 0.75 in by 0.75 in using a diamond blade, and a razor blade was used to create the initial crack. Scanning electron micrographs (SEMs) were obtained on some of the

compact tension fracture surfaces using a Leica 360 field emission gun scanning electron microscope operating at 15 kV. Secondary and back-scattering images were obtained.

Resin strength, modulus, and strain to failure were obtained by ASTM D790 three-point flexure testing using an Instron 1123 with a crosshead travel setting of 0.05 in/min. A 12:1 span-to-depth ratio for 0.5-inch wide specimens at ambient and dry conditions was used. Ten specimens were tested for each resin formulation in fracture toughness and 10 for 3-point flexure.

The glass transition temperature was obtained from the  $G''$  peak maximum obtained by torsion of a rectangular bar using a dynamic temperature ramp on a Rheometric Ares rheometer. Test parameters of 0.01-percent strain, a frequency of 100 rad/s, and a heating rate of 2°C/min were used.

## 1.4 RESULTS AND DISCUSSION

Fracture toughness results,  $K_{Ic}$ , for the control panels shown in Table 3, had an average value of 729  $\text{psi}\cdot\text{in}^{0.5}$ . Panel TG766-38-B, which contained silane coupling agent, gave the lowest fracture toughness value.

**Table 3**  
**Mechanical Data of Control Panels**

Panel #	$K_{Ic}$ , $\text{psi}\cdot\text{in}^{0.5}$
TG766-38-B	699 [49]
TG766-38-C	755 [121]
TG766-42	733 [104]

Note: The values in brackets are test standard deviation.

Panels listed in Table 4 were made using methanol as the suspension media to disperse the 33-nm and 5- $\mu\text{m}$  spherical silica particles. The weight fraction of the silicon dioxide

**Table 4**  
**Mechanical Results of Nanocomposite Panels Containing 33 nm Spherical Particles**

<b>Panel #</b>	<b>Kq, psi*in<sup>0.5</sup></b>	<b>Strength, ksi</b>	<b>Modulus, Msi</b>	<b>Failure Strain</b>
TG766-3	681 [170]	17.3 [0.8]	0.382 [0.009]	0.087 [0.020]
TG766-6	710 [213]	17.4 [0.2]	0.381 [0.003]	0.083 [0.016]
TG766-5	603 [165]	17.1 [0.3]	0.388 [0.003]	0.106 [0.016]
TG766-4	646 [151]	15.3 [3.1]	0.383 [0.006]	0.075 [0.033]
TG766-7	708 [98]	17.0 [0.5]	0.388 [0.003]	0.087 [0.020]
TG766-8	721 [127]	17.3 [0.3]	0.384 [0.009]	0.075 [0.010]
TG766-9	696 [78]	16.1 [2.2]	0.359 [0.066]	0.092 [0.026]
TG766-10	652 [86]	16.9 [1.3]	0.389 [0.004]	0.081 [0.018]
TG766-11	531 [133]	16.4 [0.5]	0.381 [0.008]	0.089 [0.017]
TG766-12	691 [149]	16.2 [1.5]	0.383 [0.004]	0.073 [0.023]

particles ranged from 0.5 to 2.0 percent. The dispersion of silicon dioxide and methanol was not very stable, as it was observed that particles settled once stirring ceased. In addition, a strip of white precipitate was found at the bottom of most panels made with methanol. The white precipitate strip confirmed that the silica was poorly dispersed in the matrix resin. The fracture toughness of these panels was not improved. The fracture toughness was not improved with or without silane coupling agent and was not affected as the concentration of silica increased, as seen in Figure 1. Five-micrometer silicon dioxide particles exhibit no difference in fracture toughness properties as compared to the 33-nm particles at a one percent loading, as shown in Figure 2, or panel TG766-12 in Table 4. It was expected that the fracture toughness would be lower for the larger particles, which would be too large for the matrix resin to form more than interphase bridges between particles.

It was visually observed that the particle distribution was more uniform when the mixing was continued overnight. This overnight mixing was required to disperse particles in the polymer resin.

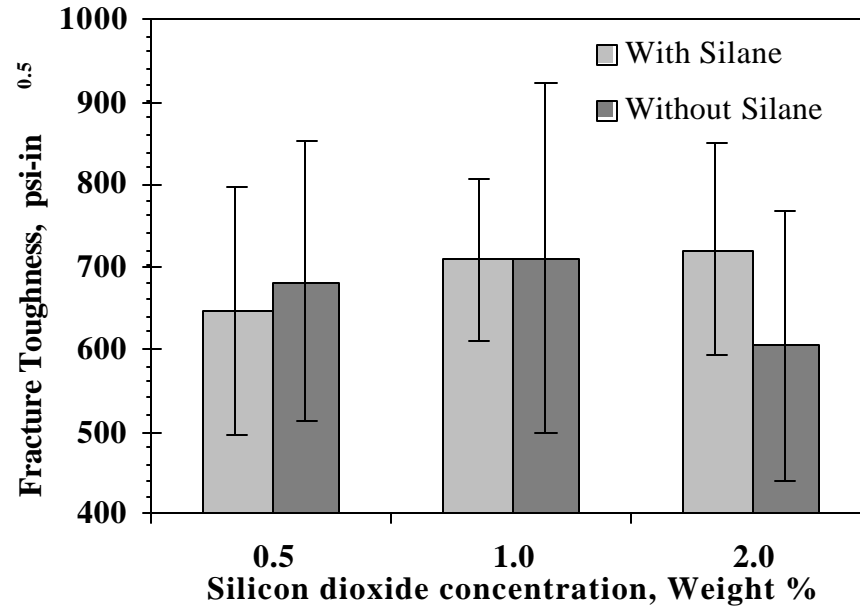


Figure 1. Fracture Toughness of 33-nm Sized Particles with or without Silane used on Different Particle Concentrations.

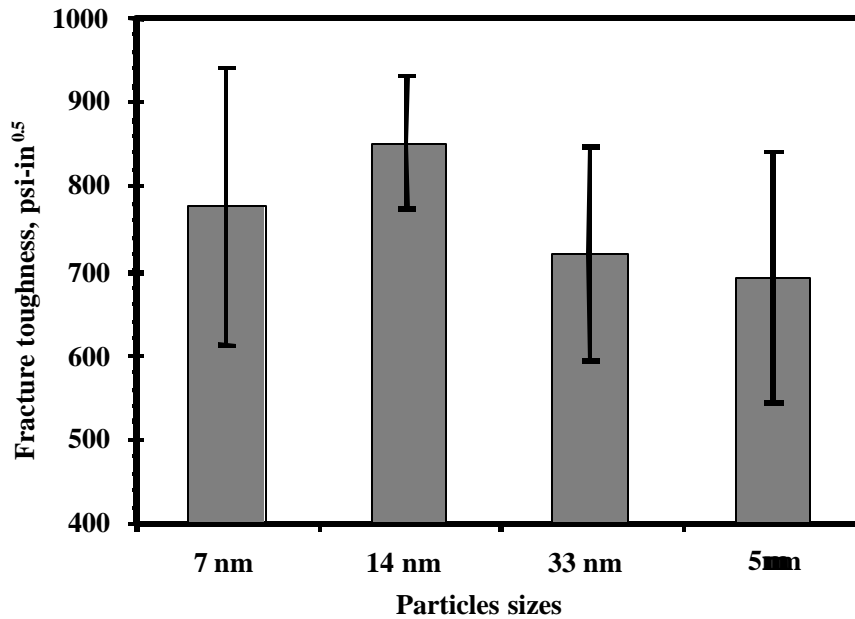


Figure 2. Fracture Toughness as a Function of Particle Size.

The 7-nm and 14-nm silica particles dispersed using acetone as a dispersion media were mixed overnight. During the course of mixing, the silica and epoxy mixture was visually observed to be well dispersed. No particle flocculation was observed in these panels, and the

panels were uniform and translucent. Fracture toughness for the panels of 14-nm particles was slightly improved as particle concentration was increased, as shown in Figure 3. A more optimized mix time of seven hours was used as shown in Table 2, versus overnight mixing of 14 nm at two percent loading. Fracture toughness was the same for the overnight mixing as seen in Table 5.

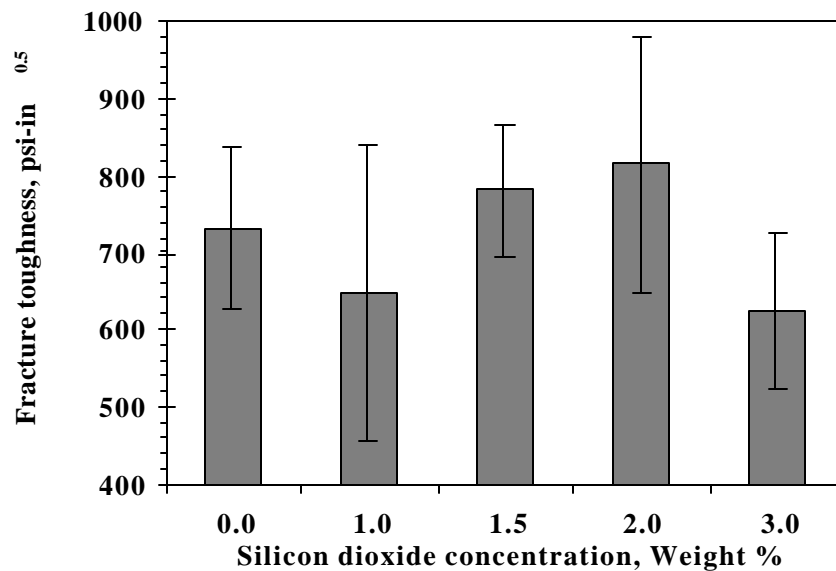


Figure 3. Fracture Toughness of 14-nm Sized Particles with Concentrations in a Range of 0 to 3%.

**Table 5**  
**Mechanical Properties of Nanocomposite Panels Containing 14-nm and 7-nm Particles**

Panel #	Kq, psi*in <sup>0.5</sup>	Strength, ksi	Modulus, Msi	Failure Strain
TG766-27S	648 [192]	17.0 [0.9]	0.370 [0.007]	0.074 [0.012]
TG766-30	781 [85]	NA	NA	NA
TG766-30-A	815 [166]	NA	NA	NA
TG766-32	815 [105]	17.1 [0.53]	0.387 [0.004]	0.093 [0.018]
TG766-34	674 [144]	16.7 [0.60]	0.372 [0.007]	0.1040 [0.02]
TG766-36	777 [86]	NA	NA	NA
TG766-38-A	721 [80]	16.1 [1.31]	0.374 [0.004]	0.0693 [0.016]
TG766-40-A	776 [166]	17.6 [0.23]	0.38 [0.006]	0.100 [0.0172]
TG766-40-B	852 [80]	16.5 [0.86]	0.377 [0.002]	0.070 [0.0107]
TG766-43-A	624 [100]	NA	NA	NA
TG766-43-B	801 [79]	NA	NA	NA
TG766-43-C	717 [119]	NA	NA	NA
TG766-43-D	814 [114]	NA	NA	NA

Note: The values in parentheses are test standard deviation.

Fracture toughness increased 22 percent at the -250°F test condition for 14-nm sized particles at a three-percent weight fraction. Panel TG766-43-A was tested at ambient temperature, and TG766-43-B was tested at -250°F (see Table 5). Panel TG766-43-C and TG766-43-D were postcured at 350°F for one hour, and it was observed that fracture toughness increased 12 percent when tested at ambient temperature, but no significant improvement was seen at the -250°F testing.

The mechanical results for panels made with silica dispersion aqueous, 20-nm particles in 40 percent water and gel silica from The Ohio State University, using acetone are shown in Table 6. Fracture toughness was low as compared to the control panels in Table 3. All panels were observed to be cloudy, and the silica particles were observed to agglomerate. A study of colloidal stability is needed for future work.

**Table 6**  
**Mechanical Results of the Suspension Particle and the Gel Particle Panels**

<b>Panel #</b>	<b>Kq, psi*in<sup>0.5</sup></b>	<b>Strength, ksi</b>	<b>Modulus, Msi</b>	<b>Failure Strain</b>
TG766-19	675.3 [86]	16.7 [0.9]	0.379 [0.006]	0.083 [0.023]
TG766-25	634 [203]	NA	NA	NA
TG766-26S	561 [158]	NA	NA	NA

Flexure strength and flexure modulus were insensitive to changes in particles sizes and loadings as shown in Figure 4.

Similarly, the glass transition temperature, T<sub>g</sub>, was not observed to change with increased silica concentration from 0.5 percent to two percent for 33-nm sized particles as shown in Table 7.

An SEM picture of the fracture surface of a composite with one-percent silicon dioxide 14-nm particles is shown in Figure 5. The particles appear to be agglomerated on the order of 100 nm. The agglomerates, however, appear to be uniformly distributed in the resin.



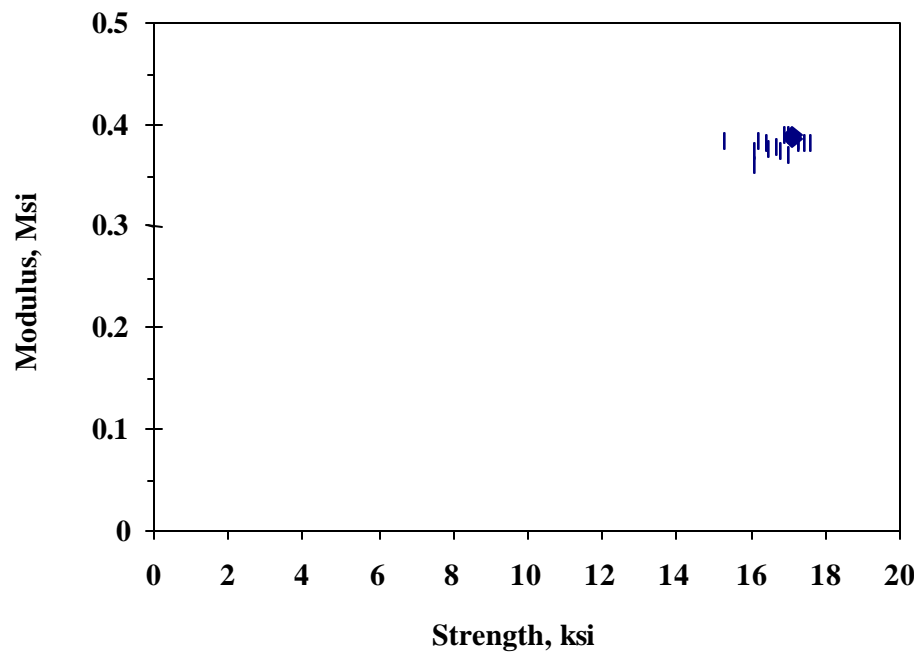


Figure 4. Flexure Modulus and Flexure Strength of Nanocomposite Panels.

**Table 7**  
**Glass Transition Temperature of 33-nm Particles**

Panel #	Concentration of Silica, % wt.	Tg, °C
TG766-4	0.5	146
TG766-7	1	145
TG766-5	2	148

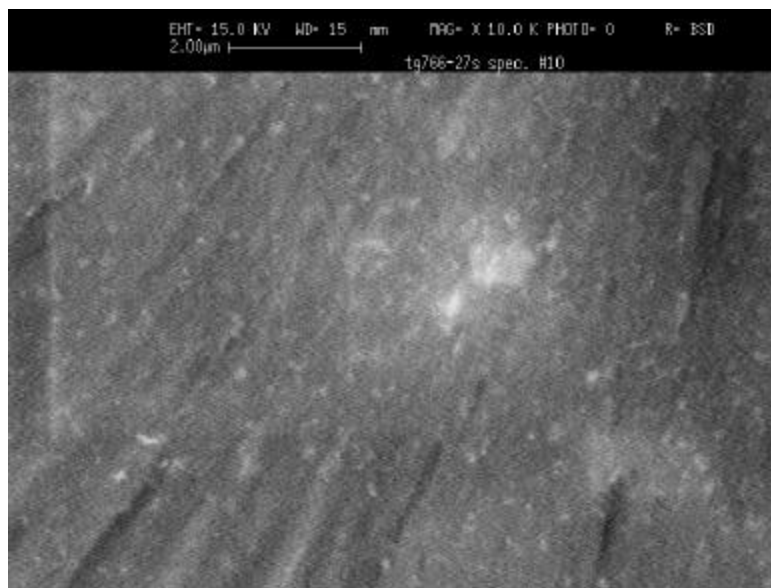


Figure 5. Scanning Electron Micrograph of 1% Silica, 14-nm Sized Panel: TG766-27S.

## 1.5 CONCLUSIONS AND RECOMMENDATIONS

For the larger nanometer-sized particles (33 nm), where methanol was used to disperse the particles, the fracture toughness was not affected by silane addition or increased silica concentration. For the 7-nm and 14-nm particles and a dispersion media of acetone, no flocculation was found, and fracture toughness was slightly improved as the particle loading was increased from one percent to two percent. Flexure strength and flexure modulus were not changed in all cases, regardless of particle size. The glass transition temperature also did not change. At this time no major trends in mechanical properties due to mixing time, particle size, or silane coupling agent were observed. The results indicated that there is a potential to improve toughness with nanoscale particles. The final properties achieved appear to be strongly correlated to the quality of the particle dispersion and thus the final morphology of the system. Optimization of the cure cycles and silica loadings is needed to improve mechanical performance.

## **2. COMMERCIAL LAYERED-SILICATE COMPOSITES**

### **2.1 INTRODUCTION**

Nanocomposites are hybrids composed of a polymer matrix and nanometer-sized inorganic reinforcement. Inorganic reinforcements used in this study include a variety of commercially available layered silicates and some in-house organoclays. The polymer matrix is Shell Epon 862, while polymerization is achieved using curing agent W as described in sections 1.2 and 1.3.

Previous research succeeded in producing several nanocomposite samples using S30A [6]. Clay loadings of three and five percent were prepared and characterized. Although S30A showed early promise at this time, attempts to replicate these results were unsuccessful. Repeatedly, S30A fell out of phase during the curing cycle. Attempts at locking the nanoparticles in phase included high-shear mixing, chemical activators, and low-temperature precure treatment (LTPT). Other organoclays were also investigated in hopes of finding one that was more compatible with the Epon 862 matrix.

### **2.2 EXPERIMENTAL PROCEDURES AND RESULTS**

#### **2.2.1 Characterization of S30A: One-Dimensional Binary Diffusion Coefficient**

The effect of adding S30A, an organoclay, to the Epon 862/W resin matrix on the absorption of water was examined. Each composite sample (see Table 8) was used to create a 2.5-mm-thick panel, from which 1-in by 1-in coupons were cut. After all coupons were dried and weighed, five coupons of each sample were placed in a 40°C water bath, and five coupons of each sample were placed in a 65°C water bath. The mass of all coupons was then taken at periodic intervals to generate mass gain versus time data. Figure 6 shows these data (the curves represent averages of five coupons).

**Table 8**  
**Composite Samples Prepared Using S30A Clay**

Sample	% Clay Loading
DC090399-0	0
DC090399-3	3
DC090399-5	5

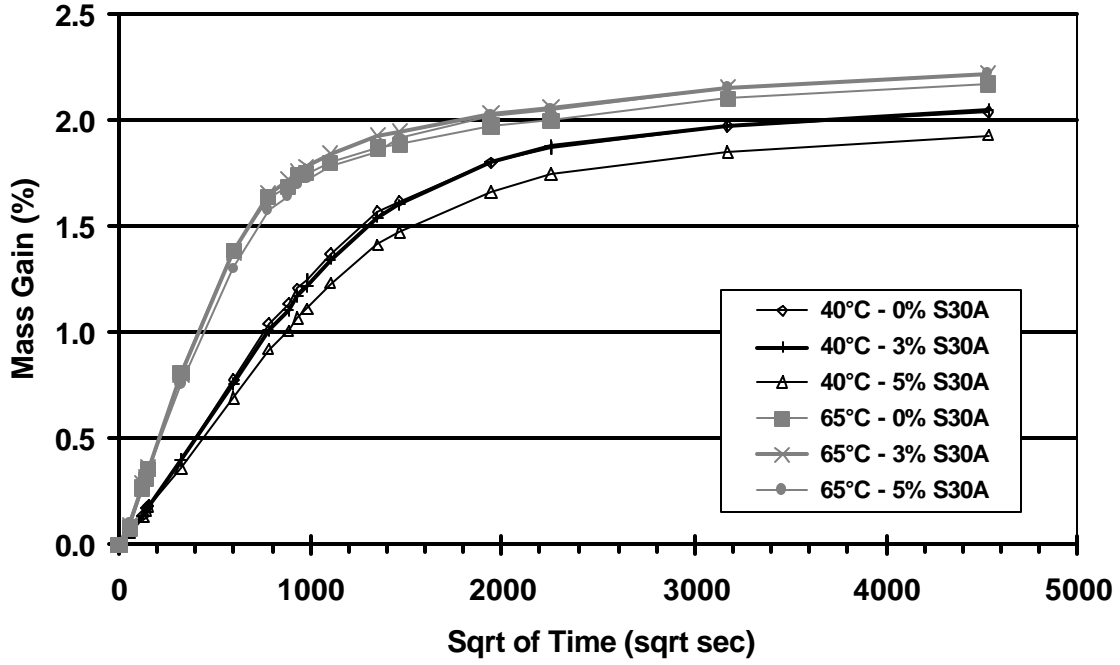


Figure 6. Mass Gains versus the Square Root of Time for the Clay Nanocomposites.

From the mass gain versus time data, the one-dimensional binary diffusion coefficient may be found from the following relationship:

$$D = \pi * [ 2 * b / (4 * M_{\max}) ]^2 * (\Delta M / \Delta t^{0.5})^2$$

D                      one-dimensional binary diffusion coefficient

b                      half-thickness

$M_{\max}$                 maximum percent mass gain

$(\Delta M / \Delta t^{0.5})$         initial slope of the mass gain versus square root of time plot

The derivation of this relationship is based on the assumption of one-dimensional diffusion, which is well justified since all coupons have an aspect ratio of approximately 20. The initial slopes of the percent mass gain versus square root of time plots were calculated using linear regression. Values for the one-dimensional binary diffusion coefficient are given in Table 9.

**Table 9**  
**Diffusion Coefficients for Each of the Composite Specimens from Figure 6**

40°C Samples		65°C Samples	
Sample #	D	Sample #	D
	(cm <sup>2</sup> /sec)		(cm <sup>2</sup> /sec)
0-1	4.8202E-09	0-4	1.4961E-08
0-2	4.8368E-09	0-5	1.4235E-08
0-3	5.0565E-09	0-6	1.4405E-08
0-9	4.8848E-09	0-10	1.4234E-08
0-14	4.9486E-09	0-19	1.4503E-08
3-3	4.6330E-09	3-1	1.3895E-08
3-5	4.6109E-09	3-4	1.3899E-08
3-9	4.5078E-09	3-8	1.3573E-08
3-12	4.6290E-09	3-11	1.3938E-08
3-18	4.7334E-09	3-13	1.3921E-08
5-2	4.3012E-09	5-1	1.2307E-08
5-5	4.3789E-09	5-3	1.2187E-08
5-6	4.2576E-09	5-4	1.1718E-08
5-9	4.3379E-09	5-7	1.2371E-08
5-16	4.3854E-09	5-19	1.1969E-08

### 2.2.2 Low-Temperature Precure Treatment (LTPT)

The effect of various curing cycles on the morphology of the S30A-Epon 862-curing agent W system was examined. Weight percents were 1.0, 78.6, and 20.4, respectively, in all trials. Dynamic mechanical analysis was used to generate viscosity-time data for the system at various temperatures (see Figure 7). Next, samples were prepared and introduced to various temperature-time ramps.

Samples (50 mL) were prepared by first adding 50 ml chloroform to one percent S30A and sonicating/mixing for one hour at 60°C. Next, Epon 862 resin was added, followed by an additional hour of sonication/mixing at 60°C. After mixing, the chloroform was removed

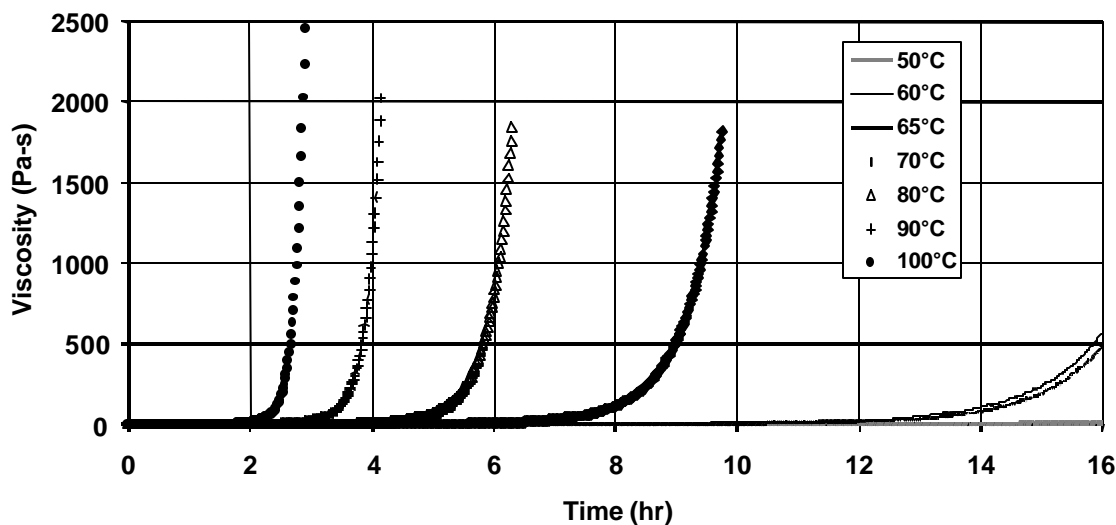


Figure 7. Viscosity-Time Data for 1% S30A-Epon 862-W.

from the S30A-Epon 862 mixture by vacuum. Curing agent W was preheated before adding and then mixed into the clay epoxy for 10 minutes. The samples were placed into small aluminum pans and cured at various temperatures and times as shown in Table 10.

**Table 10**  
**Sample Cure Cycles and Processing Observations for Small Clay Epoxy Samples**

Sample #	Cure Cycle	Observations
LC122199	4 hr @ 350°F	Flocculation occurred
LC122299	2 hr @ 250°F, 2 hr @ 350°F	Flocculation occurred
LC010600	8 hr @ 125°F, 2 hr @ 175°F	No visual flocculation
LC010700	4 hr @ 175°F	No visual flocculation
LC011100	4 hr @ 175°F	No visual flocculation

No visual flocculation occurred in three of the five samples. Although sample LC010600 showed no visual flocculation, it took 10 hours to reach a hardened state. Both LC010700 and LC0101100 displayed no flocculation while maintaining a processing time (time needed to reach a hardened state) of only four hours.

The data initially appeared to demonstrate that LTPT could be used as a means to lock the hydrophilic inorganic material in phase. Based upon this assertion, the procedure was scaled up to investigate whether the LTPT was a viable option for preventing flocculation in larger samples (300 ml). Samples were prepared identically to the smaller scaled samples. The results are given in Table 11. In every large-scale sample flocculation occurred. Precisely why LTPT prevented flocculation in small samples while failing to do so in larger samples is unclear at this time.

**Table 11**  
**Sample Cure Cycles and Processing Observations for Small Clay Epoxy Samples**

<b>Sample #</b>	<b>Cure Cycle</b>	<b>Observations</b>
LC020200	6 hr @ 175°F, 2 hr @ 250°F, 2 hr @ 350°F	Flocculation
LC020400	4 hr @ 175°F, 2 hr @ 250°F, 2 hr @ 350°F	Flocculation
LC020900	3 hr @ 167°F, 2 hr @ 250°F, 2 hr @ 350°F	Flocculation
LC020900	3 hr @ 184°F, 2 hr @ 250°F, 2 hr @ 350°F	Flocculation

### **2.2.3 Investigation of Several Commercially Available Organoclays**

Seven-layer bentonite samples were acquired from Rheox, Inc. to investigate their ability to be incorporated into Epon 862. The samples acquired were B34, B38, B52, B57, B120, BSD-1, and BSD-3. One-hundred-gram one-percent clay samples were prepared from each organoclay by first adding 100 mL acetone to 1.0 g of clay and sonicating/stirring for one hour at 60°C. Next, 78.6 g Epon 862, which had been mixing with 75 ml of acetone at 60°C for 30 min, was added to the clay/acetone and sonicated/stirred for two hours. The acetone was then evaporated off by vacuum. This step typically took 2-3 hours to complete. Curing agent W (to make 100 g total) was heated to 60°C on a hot plate and added to the clay/Epon 862, and the resulting mixture was stirred for 10 minutes.

For every bentonite clay, flocculation occurred. Additionally, every clay except BSD-1 fell out of phase immediately after the acetone was evaporated off, so the samples were not molded into plaques.

#### 2.2.4 High-Shear Mixing and the Addition of a Chemical Activator

Using three-percent S30A loading by weight in Epon 862, a qualitative analysis of the effects of the addition of a chemical activator (acetone) and the use of high-shear mixing was performed. High-shear mixing was accomplished using a Janke & Kunkel Ultra-Turrax T25 high-shear mixer at 20,500 rev/min. Acetone was added to various samples after mixing was performed, followed by several minutes of mixing using a magnetic stirring bar. Once the samples were prepared, curing agent W was added and a curing cycle of two hours at 250°F and two hours at 350°F was implemented. The samples are listed in Table 12.

**Table 12**  
**S30A Clay Composites Prepared Using High-Shear Mixing and a Chemical Activator**

Sample	Procedure	Results
A	M	Flocculation was noticeable
B	M, CA	Flocculation was noticeable, although to a lesser extent than A
C	HS	Flocculation was noticeable (similar to A)
D	M, HS	Cloudy, no noticeable aggregates
E	M, HS, CA	Cloudy, no noticeable aggregates
F	M, HS, HS, CA	Cloudy, no noticeable aggregates

M represents one hour of mixing with a magnetic stirring bar at 60°C.

CA represents the addition of a chemical activator (30% acetone relative to the S30A clay) after mixing was completed.

HS represents high-shear mixing for 10 minutes at 60°C.

First, comparing sample A to sample B, it is clear that the addition of a chemical activator aids in opening the silicate layers. Although flocculation was still present in sample B, the size of the aggregates was much smaller when compared to the aggregates formed in sample A. Comparison of sample D to sample E offers little insight visually, as both appear cloudy with no aggregates visible.



Comparing sample A to sample C, the use of 10 minutes of high-shear mixing produced similar results to one hour of mixing using a stirring bar. Both samples flocculated with large aggregates, although the processing time used was six times faster with the high-shear mixer. Comparing sample A with sample D, it is evident that high-shear mixing also aids in the opening of silicate layers, as no aggregates are visible in sample D, while large aggregates are clearly visible in sample A.

## 2.3 CONCLUSIONS

The incorporation of S30A into Epon 862 significantly decreased the one-dimensional binary diffusion coefficient of water with respect to the pristine resin matrix. Taking the arithmetic mean of each group of samples (zero-, three-, and five-percent S30A loading), it is evident that the addition of S30A to Epon 862/W decreases the one-dimensional binary diffusion coefficient appreciably (see Table 13). At 40°C, three-percent S30A loading decreases the diffusion coefficient 5.84 percent, while five-percent S30A loading decreases the diffusion coefficient 11.76 percent. At 65°C, three-percent S30A loading decreases the diffusion coefficient 4.31 percent, while five-percent S30A loading decreases the diffusion coefficient 16.3 percent.

**Table 13**  
**Average Diffusion Coefficients for S30A/Epon 862**

Sample ID	Temperature	
	40°C	65°C
	D (cm <sup>2</sup> /s)	D (cm <sup>2</sup> /s)
0% S30A	4.9094E-09	1.4468E-08
3% S30A	4.6228E-09	1.3845E-08
5% S30A	4.3322E-09	1.2110E-08

Current research in the field suggests that successful incorporation of a layered silicate into a polymer matrix depends to a great extent on the polarities of each. Commercially available organoclays typically consist of smectite clays, which have undergone ion exchange

reactions with alkylammonium ions. The addition of the alkylammonium ions increases the organic character of the clay to match more closely the organic character of the polymer. The presence of many alkyl chains in the clay galleries also tends to hydrophobize the typically inorganic silicate – this, in conjunction with the inability to successfully incorporate S30A into Epon 862 (most likely the result of manufacturer inconsistencies). Several options were available. The processing conditions could be changed so that the S30A was locked in phase, attempts to incorporate other organoclays could be made, or alternate mixing techniques could be utilized.

The first option (called LTPT) was investigated based on earlier successes in the incorporation of S30A into Epon 862. It was thought that simple processing changes might be the key to preventing flocculation. In all trials the flocculation did not occur until the final curing stage. That is, the preparation of the nanocomposite material resulted in a visually homogeneous solution (although the morphology of the system was unknown) until the sample was put through its curing cycle. This observation was the basis for altering the curing cycles to lock the nanoparticles in phase. In fact, lowering the curing temperature may allow polymerization to a hardened state, while maintaining a high enough solution viscosity to prevent the “mobility” of the silicate layers to the lower energy, stacked formation. Preliminary data seemed to substantiate this hypothesis, although attempts to scale up the operation proved unsuccessful, as flocculation occurred in all larger sample trials. Further investigation is needed to better understand these results.

With LTPT showing little hope for solving the tendency of the S30A to flocculate, attention shifted to finding a more compatible organoclay for Epon 862. Seven commercially available organoclay samples were acquired from Rheox, Inc., including B34, B38, B52, B57,

B120, BSD-1, and BSD-3. All samples displayed various tendencies to flocculate, with BSD-1 flocculating the least. However, even BSD-1 flocculated to a greater extent when compared with S30A.

High-shear mixing was also investigated as a possible solution to overcoming flocculation of the layer silicates. In order for the silicate layers to separate, energy is needed. Energy sources include chemical, thermal, and mechanical. The chemical energy was provided by use of a chemical activator such as acetone. All mixing took place at 60°C, providing thermal energy. Mechanical stirring devices provided mechanical energy. When mechanical energy increased by using a high-shear mixer, the extent of flocculation decreased. This observation was qualitative only.

The lack of success using commercial clays, combined with the successes using in-house modified clays, has led to focusing research in the synthetically modified clays discussed in the next section.

### **3. SYNTHETICALLY MODIFIED LAYERED-SILICATE COMPOSITES**

#### **3.1 INTRODUCTION**

Nanocomposites are new hybrid materials of polymers with nanometer-sized inorganic particles. Because of the unique nanometer-sized dispersion of the inorganic particles in the polymer matrix, even at very low loading of inorganic particles, these materials generally exhibit significant improvements in mechanical properties, thermal stability, barrier performance, flame retardancy, etc., compared with the base polymer [7-12]. The low loading of inorganic particles makes the conventional polymer processing such as injection molding and matrix modifications for fiber-reinforced composites possible.

The most widely used inorganic particles in polymer nanocomposites are layered silicates. Layered-silicate polymer nanocomposites have two distinct morphologies: (a) intercalated nanocomposite, in which the matrix polymer is intercalated between the silicate layers, while the expanded silicate layers are still in order; and (b) exfoliated nanocomposite, in which individual silicate layers are completely separated and dispersed in a continuous polymer matrix. The high aspect ratio and high strength of the nanoscaled layered silicate plays a key role in the improvement of the properties of the nanocomposites. The dispersion of the individual nanosheets of the layered silicates in the polymer matrix and the interfacial coupling between the individual sheets and the polymer matrix should facilitate the stress transfer to the reinforcement phase so as to improve the mechanical properties. The hindered diffusion pathways through the nanocomposite caused by the dispersion of the individual sheets of the layered silicate makes the nanocomposite exhibit the enhanced barrier properties, the resistance to the solvent uptake, reduction of thermal expansion, and flame retardances.

The most widely used layered silicate is montmorillonite, in which the backbone is a triple layer composed of two silica tetrahedral sheets fused to an edge-shared octahedral sheet of alumina or magnesium. However, the individual sheets in the silicates are generally stacked together and hydrophilic, and thus are not compatible with the hydrophobic organic matrix polymer. Therefore, the key to making a nanocomposite is to make the layered silicates compatible with the matrix polymer so that individual sheets can be separated to some extent and dispersed in the polymer matrix. The surface of the individual sheet of the layered silicate can be modified with surfactants such as alkylammonium salt through the ion exchange process to become compatible with the matrix polymer. In addition, the introduction of organic onium ions with long alkyl chains on the gallery surface of the layered silicate expand the clay gallery. This reduces the interaction between the individual sheets and also eases the penetration of the polymer or polymer precursors into the gallery. So when the interfacial interaction between the polymer and layered organosilicate is strong enough, the intercalated or exfoliated nanocomposites will be made. Until now, extensive research on the polymer layered-silicate nanocomposites was carried out [7-12]. In this current research, the emphasis is placed on epoxy-silicate nanocomposites, and especially on an aerospace epoxy system, which will also lay a foundation for developing epoxy-silicate nanocomposites as the matrix in polymer matrix composites (PMC).

## **3.2 EXPERIMENTAL PROCEDURES**

### **3.2.1 Materials**

The resins, cure agents and chemical modifiers used in this research include Shell Epon 862 (a bis-phenol F epoxy), Shell Epon 828 and Shell Epon 825 (bis-phenol A epoxies), Epi-Cure curing agent W, polyoxypropylene diamines (Jeffamine D2000, Jeffamine D400,

Jeffamine D230 and Jeffamine T430, all provided by Huntsman), *n*-octadecylamine and *n*-hexadecylamine (provided by Aldrich), and 3-cyanopropyldimethylchlorosilane and trimethylchlorosilane (provided by Gelest).

Layered silicates include Apophyllite (provided by Gelest), SNA, S30B, S10A, S6A, and S25A (all obtained from Southern Clay Products), and I.30E, I.28E, and I.22E (all obtained from Nanocor).

### **3.2.2 Preparation**

Organoclay SC16, as an example, was prepared using the following procedure. SNA was added to the solution of *n*-hexadecylamine and aqueous hydrochloric acid. The suspended mixture was stirred at elevated temperatures. The suspension was filtered. The solid was washed with solvent and dried in a vacuum oven overnight.

Organosilicate derived from apophyllite A-CM<sub>2</sub>, as an example, was prepared in the following procedure. Apophyllite was added to the 3-cyanopropyldimethylchloro-silane solution. The mixture was refluxed. The mixture was filtered and the solid was washed and dried in a vacuum oven.

### **3.2.3 Processing**

*Direct method:* The desired amount of organosilicate was added to 350 g of epoxy resin, such as Epon 862. The mixture was stirred at elevated temperature with a magnetic stir bar. Then the curing agent, such as curing agent W (91 g), was added to the mixture as the mixture was being stirred. The resulting mixture was cast between glass plates spaced 0.25 inch apart, and the mixture was then cured. The curing cycle used was the same as the standard cure cycle in section 1.3: a 30-minute ramp from ambient to 121°C, a two-hour hold at 121°C, a

30-minute ramp from 121°C to 177°C, and a two-hour hold at 177°C. The panel was cooled from 177°C to ambient temperature over two hours.

*Solvent-assisted method:* The epoxy resin was dispersed in solvent such as acetone, and the mixture was mechanically stirred and sonicated to completely disperse. The desired amount of organosilicates was added to the above mixture, and the mixture was mechanically stirred and sonicated for about two hours. Then the curing agent was added. The system was held under the vacuum to remove the solvent that had been used to help disperse the organosilicate particles, while the mechanical stirring and sonication continued. Then the resulting mixture was cast to the mold and cured in the oven. For Epon 862 and curing agent W, the curing cycle is the same as above.

#### **3.2.4 Characterization**

Thermal analysis was performed on a TA Instruments differential scanning calorimeter (DSC) 2920 modulated DSC, a TA Instruments 2940 thermomechanical analyzer (TMA) and a TA Instruments Hi-Res-TGA 2950 thermogravimetric analyzer at 10°C/min with nitrogen sweep gas. Infrared spectra was recorded on a Nicolet MAGNA-IR 560 spectrometer. Wide-angle x-ray diffraction (WAXD) was performed on a Rigaku x-ray powder diffractometer. The generator power was 40 kV and 150 mA, with a CuK $\alpha$  radiation; the scan mode is continuous with a scan rate of 0.6°/min. The sources slit (0.5°) was used for lowest possible 2 $\theta$  resolution. The scan 2 $\theta$  range is from 1.95° to 10°. Some of the small-angle x-ray scattering (SAXS) was taken with a Rigaku RU-200 statton camera. The target is CuK $\alpha$  with a wavelength of 1.5418 Å. The power is 50 kV and 150 mA. The exposure time was around 20 hours. Some of the SAXS was performed at National Synchrotron Light Source in the Brookhaven National Laboratory using a Beamline X27C with a one-dimensional detector.

The samples for transmission electron microscopy (TEM) were microtomed in a Reichert-Jung Ultracut Microtome and mounted on 200 mesh copper grids. The TEM was performed on a Phillips CM200 transmission electron microscope. The dynamic mechanical analysis was taken using Rheometrics Dynamic Spectrometer II at a frequency of 100 rad/sec, a strain of one percent, and a heating rate of 2°C/min. Resin strength, modulus, and strain-to-failure were measured under ambient conditions using a three-point flexure test configuration on an Instron load frame with a crosshead travel of 0.13 cm/min. Ten specimens were tested for each resin sample. Fracture toughness,  $K_{Ic}$ , was measured under ambient conditions and -250°F using standard compact tension described in the ASTM standard E399. Ten specimens were tested for each resin sample.

### **3.3 RESULTS AND DISCUSSION**

#### **3.3.1 Organosilicates**

The preparation of the organoclay is based on the ion-exchanged reaction, during which the ammonium onium ( $C_{16}H_{33}NH_3^+$  or  $C_{18}H_{37}NH_3^+$ ) replaces the original cations in the galleries of the clay. The preparation of the organosilicate derived from apophyllite was derived from the Lentz reaction [13], during which the organic pendent group is grafted on the gallery surface of the layered silicate by a silylation reaction. Apophyllite ( $KCa_4Si_8O_{20}(F,OH) \cdot 8H_2O$ ) is a natural silicate that has silicate sheets composed of fused 8-membered and 16-membered rings [14,15]. The pendent oxygen atoms of the 8-membered rings point alternately up and down. Apophyllite is a single-layered silicate, while montmorillonite is a tri-layered aluminum silicate.

Both synthesized organoclays and organosilicates derived from apophyllite can be characterized by WAXD and infrared (IR) spectra. The interplanar spacing of the organosilicate should be different from the original silicate, since the gallery of the silicate has been exchanged



with long alkyl chains or grafted with an organic group. In addition, IR will demonstrate that the organic group has been exchanged or grafted in the organosilicates. For example, the organosilicate A-CM<sub>2</sub> has an adsorption at 2957 cm<sup>-1</sup> and 2246 cm<sup>-1</sup>, which arises from the adsorption of CH band and CN band from the grafted organic group of the 3-cyano-propyldimethylsiloxyl pendent group. Of course, the SiO band (1057 cm<sup>-1</sup>) from the silicate backbone can always be found in IR of the organosilicates. The interaction between the organic groups and sheet silicate in the organoclay and organosilicate derived from apophyllite are different. In the organoclay, the alkylammonium pendent group just has ionic interactions with the sheet silicate anions and does not have strong covalent-bonding interaction, while the interaction between the organic groups and sheet backbone in the organosilicate derived from apophyllite have strong covalent bonds

These covalent bonds are what make the organosilicates more thermally stable. This was confirmed by the TGA data. The TGA shows that the decomposition temperatures for A-M<sub>3</sub> and A-M<sub>3</sub>-CM<sub>2</sub> are around 450°C, while the organoclay I.30E is around 260°C under nitrogen. These synthetic organosilicates derived from apophyllite should show great advantage for the polymer nanocomposites requiring high-temperature synthetic or processing procedures. A series of commercial clays and synthesized, layered organosilicates were used to make the epoxy-silicate nanocomposites. The samples and x-ray diffraction d-spacings are listed in Table 14. The layered organosilicates, which are compatible with the epoxy resin [Epon 862 with curing agent W, Epon 828 with one of the Jeffamine series, or Epon 862 or Epon 828 with nadic-methyl-anhydride (NMA) and benzyldimethylamine (BDMA)], includes SC18, SC16, I.30E, S30B, S10A and A-CM<sub>2</sub>.

**Table 14**  
**XRD Results for Nanocomposites made from Commercial and Synthesized Organosilicates**

Clay	d-spacing (Å)	Type
SNa	10.5	Sodium montmorillonite (S-series)
S30B	17.7	S-series w/ relatively strong hydrophilic organic groups
S10A	18.4	S-series w/ relatively medium hydrophilic organic groups
S25A	19.4	S-series w/ balanced hydrophobic and hydrophilic groups
S6A	35.3/19.0/12.3	S-series w/ very strong hydrophobic groups
SC16	18.2	Exchanged w/ SC <sub>16</sub> H <sub>33</sub> NH <sub>2</sub> + HCl
SC18	~18.0	Exchanged w/ SC <sub>18</sub> H <sub>37</sub> NH <sub>2</sub> + HCl
SD400	15.8	Exchanged w/ D-400 + HCl
PGW	11.9	Sodium montmorillonite w/high CEC (145 meq/100g) (Nancor)
I.30E	22.6/11.0	Nanocor
Apophyllite	7.7	KCa <sub>4</sub> Si <sub>8</sub> O <sub>20</sub> ·8H <sub>2</sub> O
A-M <sub>3</sub>	14.1	Sheet organosilicate w/ trimethylsiloxy group (nonpolar)
A-M <sub>3</sub> -CM <sub>2</sub>	16.1	Sheet organosilicate w/ mixed pendent groups (medium polar)
A-CM <sub>2</sub>	19.0	Sheet organosilicate w/ strong polar pendent siloxy group

### 3.3.2 Epoxy-Silicate Nanocomposites

A series of epoxy-silicate nanocomposites were successfully prepared. The composition, WAXD characterization, and optical appearance of the nanocomposites are listed in Table 15. The solvents used to help the layered-silicate particles disperse in some of the preparations include acetone, chloroform, tetrahydrofuran, toluene and N,N-dimethylformamide. Among them, acetone seems better than others because of good compatibility, low boiling point, and relatively low toxicity. This research also shows that the direct method of preparation of the nanocomposites without solvents is also very successful, which will eliminate the solvent removal step completely. Generally, in the nanocomposite composition, the clay loading is low, generally lower than 10 percent. However, solvent is necessary for the preparation of composites/nanocomposites with high clay loading (>10 percent). The flocculation problem in the panel sample preparation has been solved. All of the nanocomposite panel samples that were prepared appear uniform and homogeneous. The optical appearance of some nanocomposites is transparent.

**Table 15**  
**Composition, XRD Characterization and Optical Appearance of the Nanocomposites**

Resin	Curing Agent	Solvent	Clay	WAXD Characterization	Optical Appearance
862	W	NA	1.0% I.30E	Exfoliated	Transparent
862	W	NA	2.0% I.30E	Exfoliated	Transparent
862	W	NA	3.0% I.30E	Exfoliated	Transparent
862	W	NA	4.3% I.30E	Exfoliated	Translucent
862	W	NA	5.0% I.30E	Exfoliated	Translucent
862	W	NA	6.0% I.30E	Exfoliated	Translucent
862	W	NA	7.0% I.30E	Ordered Intercalated (d: 38.4/18.8/12.5Å)	Translucent
862	W	NA	10% I.30E	Ordered Intercalated (d: ~40/19.6/12.7Å)	Cloudy
862	W	NA	1.0% SC16	Exfoliated	Transparent
862	W	NA	2.1% SC16	Exfoliated	Transparent
862	W	NA	3.0% SC16	Exfoliated	Transparent
862	W	NA	3.4% SC16	Exfoliated	Transparent
862	W	NA	5.3% SC16	Exfoliated	Transparent
862	W	NA	6.0% SC16	Exfoliated	Transparent
862	W	NA	7.2% SC16	Exfoliated	Transparent
862	W	NA	1.0% SC18	Exfoliated	Transparent
862	W	NA	3.0% SC18	Exfoliated	Transparent
862	W	NA	6.0% SC18	Exfoliated	Transparent
862	W	NA	8.0% SC18	Exfoliated	Transparent
862	W	NA	3.8% S30A	Ordered Intercalated (d: 34.0/17.0/11.3Å)	Cloudy
862	W	NA	3.5% S30B	Ordered Intercalated (d: 33.3Å)	Translucent
862	W	NA	5.6% S30B	Ordered Intercalated (d: 34.0Å)	Cloudy
862	W	NA	7.0% S30B	Ordered Intercalated (d: 29.4Å)	Cloudy
862	W	NA	2.0% S10A	Ordered Intercalated (d: 31.0, 15.1Å)	Translucent
862	W	NA	5.0% S10A	Ordered Intercalated (d: 31.5, 15.2, 10.1)	Cloudy
862	W	Tol.	1.0% S30B	Partially Exfoliated (d: ~30Å)	Translucent
862	W	THF	2.0% S30B	Partially Exfoliated (d: ~30Å)	Cloudy
862	W	DMF	2.0% S30B	Partially Exfoliated (d: ~40Å)	Cloudy
862	W	Acetone	0.6% A-CM <sub>2</sub>	Exfoliated	Translucent
862	W	Acetone	2.0% A-CM <sub>2</sub>	Exfoliated	Cloudy
828	D2000	NA	5.1% I.30E	Exfoliated	Transparent
828	D400	NA	3.5% I.30E	Mostly Exfoliated	Transparent
828	D400	NA	5.1% I.30E	Mostly Exfoliated	Transparent
828	D230	NA	5.6% I.30E	Partially Exfoliated	Transparent
828	D230	NA	7.2% I.30E	Partially Exfoliated	Transparent
828	T403	NA	3.5% I.30E	Exfoliated	Transparent
828	T403	NA	4.8% I.30E	Exfoliated	Transparent
825	D230	NA	5.7% I.30E	Exfoliated	Transparent
825	D400	NA	5.0% I.30E	Exfoliated	Transparent
825	T403	NA	5.4% I.30E	Exfoliated	Transparent
825	T403	NA	5.0% I.28E	Ordered Intercalated (d: 34.7/17.1Å)	Transparent
828	NMA / BDMA	NA	1.0% I.28E	Ordered Intercalated (d: 38.5/19.2/12.6Å)	Transparent
828	NMA / BDMA	NA	3.0% I.28E	Ordered Intercalated (d: 37.6/18.2/12.1Å)	Transparent
828	NMA / BDMA	NA	4.7% I.28E	Ordered Intercalated (d: 36.8/17.9/11.9Å)	Translucent
862	NMA / BDMA	NA	1.0% I.28E	Ordered Intercalated (d: 39.7/19.8/12.6Å)	Transparent
862	NMA / BDMA	NA	2.8% I.28E	Ordered Intercalated (d: 39.3/18.8/12.2Å)	Transparent
862	NMA / BDMA	NA	4.7% I.28E	Ordered Intercalated (d: 32.7/17.0/11.5Å)	Translucent
828	MPDA	NA	5.0% I.30E	Exfoliated	Translucent
828	MPDA	NA	5.0% SC18	Exfoliated	Transparent

The most common characterization method for nanocomposites is WAXD. Since the interplanar spacing for the organosilicate is in the range of 15 to 25 Å, WAXD provides the information whether or not the nanocomposite is formed. The typical WAXD of the intercalated nanocomposite will show the shift of the interplanar spacing of the silicate to a larger interplanar spacing. In this research the WAXD data were collected from a starting angle as low as  $1.95^\circ$   $2\theta$ , which corresponds to a d-spacing value of 45 Å. So if there is no peak in the WAXD, the interplanar spacing between the silicate layers is larger than 45 Å, and it is generally assumed that the silicate sheet is expanded and separated in the epoxy resin matrix. The epoxy-silicate nanocomposites are considered to be exfoliated or mostly exfoliated.

To get a deeper understanding of the structure and morphology of the nanocomposite, SAXS of some nanocomposites without peaks in their WAXD was measured. The small-angle x-ray diffraction of Rigaku RU-200 confirms that there is a clear but weak peak at even larger interplanar spacing. More data from SAXS at the National Synchrotron Light Source at Brookhaven National Laboratory were in very good agreement with the data from Rigaku RU-200. The data are shown in Table 16. Most interplanar spacings of the nanocomposites are larger than 100 Å, and the weakness of the peak demonstrates the existence of the disordered structures. So the silicate nanosheets are evenly dispersed, and these types of morphology can be considered to be exfoliated nanocomposites. When the loading of the clay is lower (one percent SC16/Epon 862/W), the interplanar spacing of the nanosheet is increased (240 Å). This is reasonable since there is more epoxy resin between the nanosheet due to the low loading of the clay. In addition, the interplanar spacing of the nanocomposites from the synthetic organoclay (SC16 and SC18) is larger than that from commercial organoclay (I.30E), although the original interplanar spacing of the synthetic clay (~18 Å) is even smaller than that

**Table 16**  
**Composition, SAXS Data of the Nanocomposites from Rigaku RU-200 and National Synchrotron Light Source**

Epon	Curing Agent	Clay	d-Spacing (Å)	
			Rigaku	NSLS
862	W	1.0 % SC16		238
862	W	3.0 % SC16	156	151
862	W	6.0 % SC16	150	141
862	W	1.0 % SC18		249
862	W	3.0 % SC18	135	135
862	W	6.0 % SC18		129
862	W	8.0 % SC18		114
862	W	1.0 % I.30E		172
862	W	3.0 % I.30E	125	126
862	W	6.0 % I.30E	100, 48	100, 49
828	MPDA	5.0 % SC18		87, 42

of commercial organoclay (I.30E, 22.6 Å). This is perhaps caused by higher purity of synthetic organoclay, and thus better compatibility with the epoxy resin.

The *in situ* SAXS of the curing process of organoclay/epoxy resin was recorded at Brookhaven National Laboratory. The data processing is still underway. The information will be important to understanding the exfoliation process for the organoclay/epoxy system.

The TEM provides direct observation and direct evidence of the detailed features of the morphology of the polymer layered-silicate nanocomposites. Several exfoliated layered-silicate-epoxy nanocomposites were microtomed and examined by TEM. The TEM of three percent SC16/Epon 862/W in Figure 8 shows the typical morphology of the exfoliated layered-silicate-epoxy nanocomposites. The original aggregates of the silicate sheets are disrupted, and each individual sheet with nanometer-thickness is very well dispersed in the epoxy resin. Some individual sheets are completely disordered, while some still preserve the parallel alignment of layers with ~15 nm separation. This result is consistent with the SAXS results, which show a clear but weak peak at ~150 Å (15 nm).

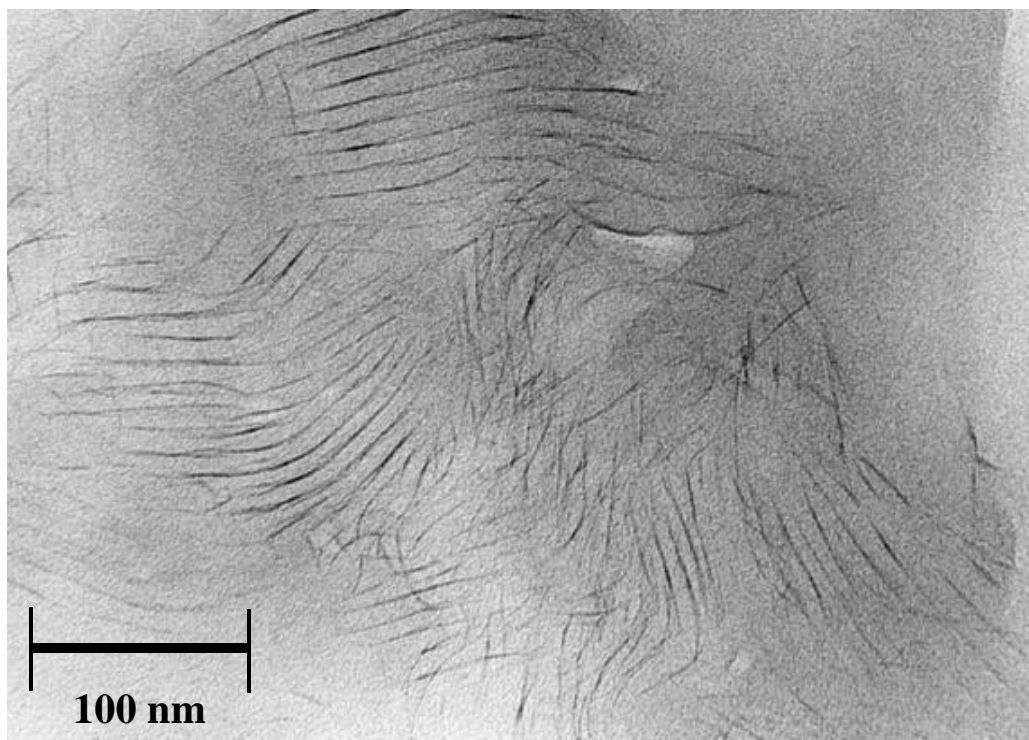


Figure 8. The TEM Micrograph of the Epoxy-Nanocomposite of 3% SC16/Epon 862/W.

The x-ray powder diffraction demonstrates that all of the nanocomposites made from the epoxy resin (Epon 862 and curing agent W) with I.30E, SC18, and SC16 are exfoliated and appear transparent or translucent. The nanocomposites made from the epoxy resin (Epon 862 and curing agent W) with S30B and S10A are ordered intercalated when the clay loading is higher than two percent, while the nanocomposites are partially exfoliated or disordered intercalated with low clay loading. The optical appearance of these nanocomposites with S-series clay are cloudy or translucent. The nanocomposites made from the epoxy resin (Epon 828 and Jeffamine D2000, D400, D230, and T403) are exfoliated or partially exfoliated and appear transparent. So the optical appearance depends on the composition of the nanocomposites (silicates, epoxy, and curing agent). Generally, the exfoliated nanocomposites show good optical

quality since the nanometer-thickness sheets of the silicate are fully separated and dispersed in the epoxy resin-matrix. The optical appearance of the nanocomposites with SC16 and SC18 is even better, which perhaps is caused by a purer quality of synthesized organoclay.

The thermal expansion coefficients of the nanocomposites and their pristine polymers are listed in Table 17. The thermomechanical analysis shows that the thermal expansion coefficients of the nanocomposites are lower than those of pristine polymer in glassy states. The reduction of the thermal expansion coefficient is perhaps due to the presence of silicate nanosheets and their constraining effect.

**Table 17**  
**Thermal Expansion Coefficients of the Nanocomposites and Their Pristine Polymers**

Epon Resin	Curing Agent	Clay	CTE, $\alpha$ ( $\mu\text{m}/\text{m}/^\circ\text{C}$ )
			(below T <sub>g</sub> )
862	W	NA	76.6
862	W	1.0% SC16	69.5
862	W	3.0% SC16	63.0
862	W	6.0% SC16	64.3
862	W	1.0% I.30E	71.3
862	W	3.0% I.30E	66.9
862	W	6.0% I.30E	64.8
862	W	1.0% SC18	73.4
862	W	3.0% SC18	61.3
862	W	6.0% SC18	64.8
862	W	8.0% SC18	61.0
862	W	NA	63.4
862	W	3.0% I.30E	56.9
862	W	4.3% I.30E	53.8

A study of the viscosity of the Epon 862 resin and curing agent W with various clay loadings (0 percent, one percent, three percent and five percent of I.30E) (Figure 9), indicates that although there are some increases in the viscosity of the resin with clay loading in the first 30 minutes (1800 seconds), the viscosity is still low enough to be processed. However, after 30 minutes, the viscosity of the epoxy resin with clay is increased significantly, and the

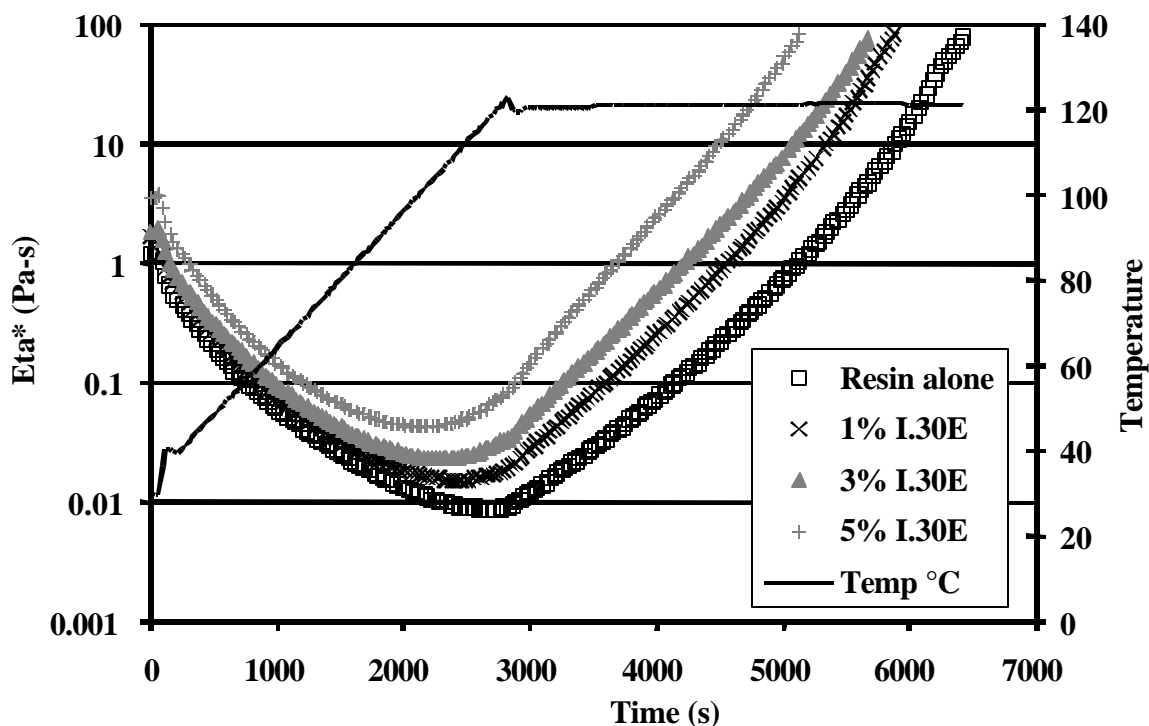


Figure 9. The Viscosity of the Epon 862 Resin and Curing Agent W with Various Clay (I.30E) Loadings (0%, 1%, 3% and 5%).

lowest viscosity positions are shifted to shorter time. This is probably related to the exfoliation process and curing procedure. The viscosity study, underway in our laboratory, together with DSC and Fourier transform infrared (FTIR) spectroscopy, will provide a deeper understanding of the kinetics of the exfoliation procedure. This can also be related to the information obtained from the *in situ* SAXS data also underway in the laboratory.

The dynamic mechanical analysis, Table 18, shows that the storage modulus of the nanocomposites is higher than that of the pristine epoxy resin. Generally, the nanocomposites show more significant improvement of storage modulus in the rubber state than that in the glassy state. This perhaps is caused by the extra reinforcement from further nanosheet alignment in the rubber state.



**Table 18**  
**Storage Moduli and Glass Transition Temperatures (T<sub>g</sub>) of the Nanocomposites and Their Pristine Polymers from Dynamic Mechanical Analysis**

Resin	Curing Agent	Clay	T <sub>g</sub> (°C) Tan $\delta$	G' (dyne/cm <sup>2</sup> )	
				Glassy	Rubber
862	W	NA	154	1.14E10 (30°C)	1.03E8 (180°C)
862	W	1.0% I.30E	153	1.20E10 (30°C)	1.24E8 (180°C)
862	W	1.0% I.30E	154	1.08E10 (30°C)	1.09E8 (180°C)
862	W	3.0% I.30E	155	1.10E10 (30°C)	1.45E8 (180°C)
862	W	6.0% I.30E	159	1.14E10 (30°C)	1.80E8 (180°C)
862	W	4.3% I.30E	158	1.26E10 (30°C)	1.91E8 (180°C)
862	W	1.0% SC16	155	1.20E10 (30°C)	1.16E8 (180°C)
862	W	3.0% SC16	154	1.18E10 (30°C)	1.63E8 (180°C)
862	W	6.0% SC16	155	1.24E10 (30°C)	2.45E8 (180°C)
862	W	3.4% SC16	153	1.15E10 (30°C)	1.51E8 (180°C)
862	W	5.3% SC16	151	1.18E10 (30°C)	1.74E8(180°C)
862	W	7.2% SC16	152	1.25E10 (30°C)	2.10E8 (180°C)
862	W	7.0% I.30E	156	1.25E10 (30°C)	1.84E8 (180°C)
862	W	3.8% S30A	155	1.38E10 (30°C)	1.60E8 (180°C)
862	W	3.5% S30B	157	1.18E10 (30°C)	1.36E8 (180°C)
862	W	7.0% S30B	161	1.33E10 (30°C)	2.05E8 (180°C)
825	T403	NA	101	1.10E10 (30°C)	0.84E8 (120°C)
825	T403	5.4% I.30E	96	1.10E10 (30°C)	1.49E8 (120°C)
825	T403	5.0% I.28E	102	1.11E10 (30°C)	1.12E8 (120°C)
828	T403	NA	100	1.00E10 (30°C)	7.60E7 (120°C)
828	T403	3.5% I.30E	101	1.27E10 (30°C)	11.7E7 (120°C)
828	D230	NA	95.9	1.05E10 (30°C)	6.52E7 (120°C)
828	D230	5.6% I.30E	92.6	1.19E10 (30°C)	9.33E7 (120°C)
828	D230	7.2% I.30E	82.5	1.30E10 (30°C)	8.74E7 (100°C)
828	D400	NA	57.7	1.06E10 (30°C)	3.56E7 (100°C)
828	D400	3.5% I.30E	56.5	1.27E10 (30°C)	4.69E7 (100°C)
828	D400	5.1% I.30E	52.5	1.18E10 (30°C)	5.11E7 (100°C)
828	D2000	NA	-19.3	1.18E10 (-100°C)	1.11E7 (30°C)
828	D2000	5.1% I.30E	-17.6	1.65E10 (-100°C)	3.12E7 (30°C)
828	NMA/BDMA	NA	159	1.19E10 (30°C)	0.93E8(180°C)
828	NMA/BDMA	1.0% I.28E	165	1.10E10 (30°C)	0.88E8(180°C)
828	NMA/BDMA	3.0% I.28E	159	1.34E10 (30°C)	1.16E8 (180°C)
828	NMA/BDMA	4.7% I.28E	169	1.24E10 (30°C)	1.43E8 (180°C)
862	NMA/BDMA	NA	144	1.31E10 (30°C)	1.06E8 (180°C)
862	NMA/BDMA	2.8% I.28E	166	1.20E10 (30°C)	1.52E8 (180°C)

The mechanical properties of some of the nanocomposite panels at room temperature are shown in Table 19, and the compact tension results of some nanocomposite panels at -250°F are shown in Table 20. The modulus of the nanocomposites is generally higher than the pristine polymer, while the fracture toughness of the nanocomposites is reduced to some extent. One interesting phenomenon is that the fracture toughness at low temperature is even

**Table 19**  
**Mechanical Properties of Nanocomposites**

<b>Panel #</b>	<b>Kq (psi * in<sup>0.5</sup>)</b>	<b>Strength (ksi)</b>	<b>Modulus (Msi)</b>	<b>Failure Strain (%)</b>
Epon 862/W	653 [237]	17.9 [1.1]	0.387 [0.012]	0.079 [0.023]
1.0% S25A/Epon 862/W	498 [42]	11.0 [2.4]	0.382 [0.007]	0.033 [0.009]
1.0% S30B/Epon 862/W	589 [59]	13.7 [1.7]	0.449 [0.003]	0.036 [0.006]
0.6% A-CM <sub>2</sub> /Epon 862/W	716 [85]	15.9 [1.2]	0.370 [0.005]	0.081 [0.091]
2.0% A-CM <sub>2</sub> /Epon 862/W	656 [153]	13.4 [3.6]	0.396 [0.017]	0.047 [0.017]
1.0% I.30E/Epon 862/W	606 [51]	14.4 [1.4]	0.355 [0.022]	0.054 [0.023]
2.0% I.30E/Epon 862/W	525 [83]	15.0 [2.1]	0.435 [0.030]	0.042 [0.009]
3.0% I.30E/Epon 862/W	472 [43]	9.1 [2.3]	0.402 [0.007]	0.025 [0.009]
4.3% I.30E/Epon 862/W	466 [99]	13.7 [2.7]	0.436 [0.004]	0.039 [0.010]
2.1% SC16/Epon 862/W	557 [51]	15.2 [1.8]	0.409 [0.005]	0.050 [0.010]
1.0% SC18/Epon 862/W	477 [37]	16.7 [1.2]	0.388 [0.004]	0.076 [0.017]
3.0% SC18/Epon 862/W	477 [49]	15.9 [1.2]	0.403 [0.013]	0.056 [0.010]
6.0% SC18/Epon 862/W	509 [40]	15.0 [1.2]	0.472 [0.007]	0.039 [0.005]
8.0% SC18/Epon 862/W	419 [42]	14.4 [1.2]	0.483 [0.005]	0.036 [0.004]

\*the numbers in brackets are standard deviation

**Table 20**  
**Compact Tension Test Results from Nanocomposites at -250°F**

<b>Panel #</b>	<b>Kq psi * in<sup>0.5</sup></b>
Epon 862/W	792 [120]
1.0% I.30E/Epon 862/W	593 [132]
3.0% I.30E/Epon 862/W	668 [73]
6.0% I.30E/Epon 862/W	604 [90]

\*the numbers in brackets are standard deviation

higher than that at room temperature. Perhaps the key to improving the toughness of the nanocomposite is to enhance the interfacial interaction between the polymer matrix and layered silicates, which will be included in later research.

Figure 10 shows the solvent uptake of the nanocomposite in methanol. The data show that the methanol uptake for the nanocomposite after 22 days is about half compared with the pristine polymer. This is also ascribed to the barrier effect of nanosheets of the nanoclay in the epoxy resin. More solvents are being tested and more information, such as diffusivity, is being studied.

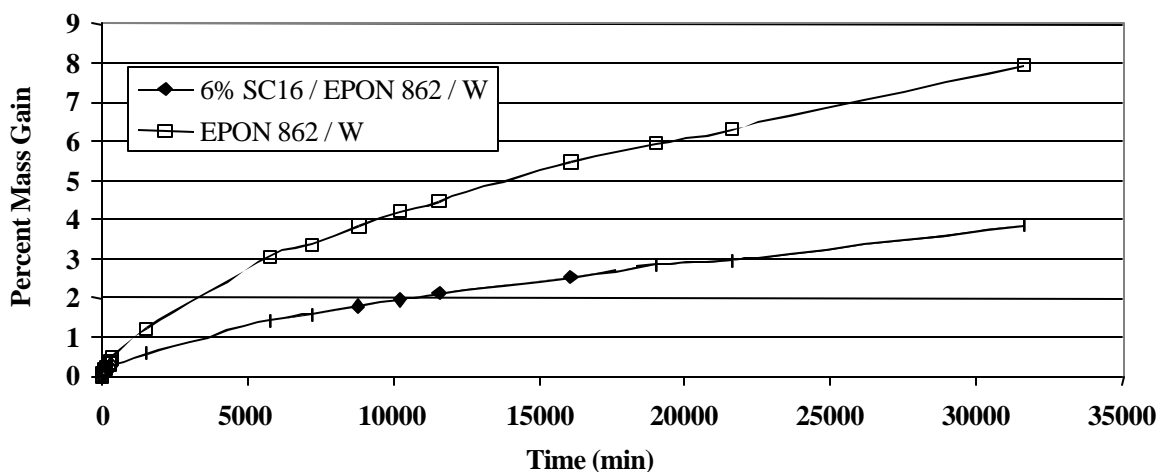


Figure 10. Uptake of 6% SC16/Epon 862/W and Epon 862/W (Control) in Methanol.

### 3.4 CONCLUSIONS

The results of this research demonstrate that commercial organoclays can be used to make epoxy nanocomposites. The desired organosilicates can also be synthesized to be compatible with the epoxy resin and used to form epoxy nanocomposites. Generally synthetic organosilicates have higher quality. The nanocomposites were characterized by WAXD, SAXS, and TEM. The TEM of the nanocomposites directly shows that the organoclay was very well dispersed in the epoxy resin. The results of the transmission electron microscope are consistent with the results of the SAXS data. The epoxy-nanocomposite shows reduced thermal expansion coefficients, higher modulus, lower fracture toughness and reduced solvent uptake. Perhaps the critical key for improving the toughness of the nanocomposite is to enhance the interface interaction by chemical covalent bonding. This will be the focus of future research. In addition, the incorporation of I.30E/Epon 862/W nanocomposite as a matrix into carbon fiber-reinforced composites will be attempted.

#### 4. PUBLICATIONS AND PRESENTATIONS

The following publications and/or presentations were generated during this reporting period.

Chen, C., D. P. Anderson, & D. B. Curliss. (2000). Characterization of a Series of Glassy Epoxy-Silicate Nanocomposites. *ACS Polymer Preprints* 41(1) (523).

Anderson, D. P., T. Gibson, & T. Benson Tolle. (2000, March). *The Effects of Nanoscale Inorganic Fillers on an Aerospace Epoxy Resin*. AIAA 25<sup>th</sup> Dayton-Cincinnati Aerospace Science Symposium.

Anderson, D. P., T. Benson Tolle, & T. Gibson. (2000). Composite Property Enhancement with Nanoscale Inorganic Fillers. *Proc. of ACS PMSE* 82 (220).

Chen, C., & D. B. Curliss. (2000). *Preparation, Characterization and Properties of the Aerospace Epoxy Layered-Silicate Nanocomposite*. 1<sup>st</sup> Georgia Tech Conference on Nanoscience and Nanotechnology, Atlanta, GA.

## 5. REFERENCES

1. Okada, A., M. Kawasumi, T. Kurauchi, & O. Kamigaito. (1987). Synthesis and Characterization of a Nylon-6 – Clay Hybrid. *Polymer Preprints* 28 (447).
2. Kojima, Y., A. Usuki, M. Kawasumi, A. Okada, Y. Fukushima, T. Kurauchi, & O. Kamigaito. (1993). Mechanical Properties of Nylon-6 – Clay Hybrid. *J. Mater. Res.* 8 (1185).
3. Shi, H., T. Lan, & T. J. Pinnavaia. (1996). Interfacial Effects on the Reinforcement Properties of Polymer-Organoclay Nanocomposites. *Chem. Mater.* 8 (1584).
4. Anderson, D. P., T. Benson Tolle, & T. Gibson. (2000). Composite Property Enhancement with Nanoscale Inorganic Fillers. *Proc. of ACS PMSE* 82 (220); and Anderson, D. P., T. Gibson, & T. Benson Tolle. (2000, March). *The Effects of Nanoscale Inorganic Fillers on an Aerospace Epoxy Resin*. Presented at the 25<sup>th</sup> AIAA Dayton-Cincinnati Aerospace Science Symposium.
5. Anderson, D. P., & B. P. Rice. (2000). *Intrinsically Survivable Structural Composite Materials* (AFRL-ML-WP-TR-1999-4016). Dayton, OH: U.S. Air Force.
6. Chen, C., D. P. Anderson, & D. B. Curliss. (2000). Characterization of a Series of Glass Epoxy-Silicate Nanocomposites. *ACS Polymer Preprints* 41(1) (523).
7. Giannelis, E. P. (1996). Polymer-Layered Silicate Nanocomposites. *Advanced Materials* 8(1) (29).
8. Giannelis, E. P. (1998). Polymer-Layered Silicate Nanocomposites: Synthesis, Properties and Applications. *Appl. Organometal. Chem.* 12 (675).
9. LeBaron, P. C., Z. Wang, & T. J. Pinnavaia. (1999). Polymer-Layered Silicate Nanocomposites: an Overview. *Applied Clay Science* 15 (11).
10. Gilman, J. W. (1999). Flammability and Thermal Stability Studies of Polymer-Layered Silicate (Clay) Nanocomposites. *Applied Clay Science* 15 (31).
11. Porter, D., E. Metcalfe, & M. J. K. Thomas. (2000). Nanocomposite Fire Retardants – A Review. *Fire Mat.* 24 (45).
12. Alexandre, M., & P. Dubois. (2000). Polymer-Layered Silicate Nanocomposites: Preparation, Properties and Use of a New Class of Materials. *Materials Science and Engineering* 28 (1).
13. Lentz, C. W. (1964). Silicate Minerals as Sources of Trimethylsilyl Silicates and Silicate Structure Analysis of Sodium Silicate Solutions. *Inorg. Chem.* 3 (574).

14. Colville, A. A., C. P. Anderson, & P. M. Black. (1971). Refinement of Crystal Structure of Apophyllite, I. X-ray Diffraction and Physical Properties. *Am. Miner.* 56 (1222).
15. Pechar, F. (1987). An X-ray Diffraction Refinement of the Crystal Structure of Apophyllite. *Cryst. Res. Technol.* 22 (1041).

## LIST OF ACRONYMS

<b><u>Acronym</u></b>	<b><u>Description</u></b>
ACS	American Chemical Society
ASTM	American Society for Testing and Materials
BDMA	benzyl dimethylamine
DMF	N,N-dimethylformamide
DSC	differential scanning calorimeter
FTIR	Fourier transform infrared
LTPT	low-temperature precure treatment
MPDA	m-phenylene diamine
NMA	nadic-methyl-anhydride
NSLS	National Synchrotron Light Source
PMC	polymer matrix composites
RTM	resin transfer molding
SAXS	small-angle x-ray scattering
SEM	scanning electron micrograph
TGA	thermogravimetric analyzer
TMA	thermomechanical analyzer
THF	tetrahydrofuran
T <sub>g</sub>	transition temperature
WAXD	wide-angle x-ray diffraction